Impact of Pavement Friction on Traffic Safety, Phase I: Pavement Friction Evaluation

Final Report
July 2025

ctre
Center for Transportation Research and Education

IOWA STATE UNIVERSITY
Institute for Transportation

Sponsored by
Iowa Department of Transportation
(InTrans Project 19-719)
Federal Highway Administration

About the Center for Transportation Research and Education

The mission of the Center for Transportation Research and Education (CTRE) at Iowa State University is to conduct basic and applied transportation research to help our partners improve safety, facilitate traffic operations, and enhance the management of infrastructure assets.

About the Institute for Transportation

The mission of the Institute for Transportation (InTrans) at Iowa State University is to save lives and improve economic vitality through discovery, research innovation, outreach, and the implementation of bold ideas.

Iowa State University Nondiscrimination Statement

Iowa State University does not discriminate on the basis of race, color, age, ethnicity, religion, national origin, pregnancy, sexual orientation, genetic information, sex, marital status, disability, or status as a U.S. Veteran. Inquiries regarding nondiscrimination policies may be directed to Office of Equal Opportunity, 2680 Beardshear Hall, 515 Morrill Road, Ames, Iowa 50011, telephone: 515-294-7612, email: eooffice@iastate.edu.

Disclaimer Notice

The contents of this report reflect the views of the authors, who are responsible for the facts and the accuracy of the information presented herein. The opinions, findings and conclusions expressed in this publication are those of the authors and not necessarily those of the sponsors.

The sponsors assume no liability for the contents or use of the information contained in this document. This report does not constitute a standard, specification, or regulation.

The sponsors do not endorse products or manufacturers. Trademarks or manufacturers' names appear in this report only because they are considered essential to the objective of the document.

Quality Assurance Statement

The Federal Highway Administration (FHWA) provides high-quality information to serve Government, industry, and the public in a manner that promotes public understanding. Standards and policies are used to ensure and maximize the quality, objectivity, utility, and integrity of its information. The FHWA periodically reviews quality issues and adjusts its programs and processes to ensure continuous quality improvement.

Iowa DOT Statements

Iowa DOT ensures non-discrimination in all programs and activities in accordance with Title VI of the Civil Rights Act of 1964. Any person who believes that they are being denied participation in a project, being denied benefits of a program, or otherwise being discriminated against because of race, color, national origin, gender, age, or disability, low income and limited English proficiency, or if needs more information or special assistance for persons with disabilities or limited English proficiency, please contact Iowa DOT Civil Rights at 515-239-7970 or by email at civil.rights@iowadot.us.

The preparation of this report was financed in part through funds provided by the Iowa Department of Transportation through its "Second Revised Agreement for Management of Research Conducted by Iowa State University for the Iowa Department of Transportation" and its amendments.

The opinions, findings, and conclusions expressed in this publication are those of the authors and not necessarily those of the Iowa Department of Transportation or the U.S. Department of Transportation Federal Highway Administration.

Technical Report Documentation Page

1. Report No.	2. Government Accession No.	3. Recipient's Catalog No.
InTrans Project 19-719		

4. Title and Subtitle	5. Report Date
Impact of Pavement Friction on Traffic Safety, Phase I: Pavement Friction Evaluation	July 2025
	6. Performing Organization Code

7. Author(s)	8. Performing Organization Report No.
Omar Smadi (orcid.org/0000-0002-3147-9232), Ahmad Alhasan (orcid.org/0000-0002-0091-9899), and Alireza Sassani (orcid.org/0000-0002-8140-0246)	InTrans Project 19-719

9. Performing Organization Name and Address	10. Work Unit No. (TRAIS)
Center for Transportation Research and Education Iowa State University 2711 South Loop Drive, Suite 4700 Ames, IA 50010-8664	11. Contract or Grant No.

12. Sponsoring Organization Name and Address		13. Type of Report and Period Covered
Iowa Department of Transportation 800 Lincoln Way Ames, IA 50010	Federal Highway Administration 1200 New Jersey Avenue, SE Washington, DC 20590	Final Report
		14. Sponsoring Agency Code 20-SPR0-008

15. Supplementary Notes

Visit https://ctre.iastate.edu for color pdfs of this and other research reports.

16. Abstract

Pavement friction significantly contributes to roadway safety by providing the grip required for safe travel. The Iowa Department of Transportation (DOT) has long recognized the importance of evaluating pavement skid resistance and its impact on traffic safety.

Several devices have been developed to measure skid resistance. The Iowa DOT currently uses the locked-wheel skid tester (LWST), which is well accepted across the United States and globally. Due to its relatively narrow speed range and limitations on curves and short, low-speed segments, various types of continuous friction measurement equipment (CFME) have been proposed as alternatives, including the GripTester and sideway-force coefficient routine investigation machine (SCRIM). A broader issue in friction measurement is repeatability and reliability under different operational conditions, with temperature, pavement wetting, and test speed affecting the correlation between different devices.

This study aimed to evaluate candidate CFME technologies for their ability to measure pavement friction at different test speeds and in different operational conditions relative to the LWST currently available at the Iowa DOT. Promising CFME technologies were selected, and a testing program based on statistical procedures was designed to evaluate the devices' suitability for pavement friction evaluation in relation to the friction demand and safety analysis. CFME and LWST testing was performed at three asphalt and three concrete pavement test segments at different speeds and using smooth and ribbed tires, and tests were repeated on different days to determine performance in different operational conditions. A dynamic friction tester (DFT) and laser texture scanner (LTS) were used to verify the correlation between the CFME and LWST and to investigate the impact of pavement texture on dry and wet skid resistance.

The research resulted in guidance and recommendations for friction evaluation on different components of the network, including curves and low-speed segments. These outcomes represent a step toward a consistent procedure for both routine pavement friction evaluation at the network level and spot investigation for high-risk areas.

17. Key Words	18. Distribution Statement
continuous friction measurement equipment—locked-wheel skid tester—pavement friction—pavement texture—skid resistance	No restrictions.

19. Security Classification (of this report)	20. Security Classification (of this page)	21. No. of Pages	22. Price
Unclassified.	Unclassified.	82	NA

IMPACT OF PAVEMENT FRICTION ON TRAFFIC SAFETY, PHASE I: PAVEMENT FRICTION EVALUATION

Final Report
July 2025

Principal Investigator
Omar Smadi, Director
Center for Transportation Research and Education, Iowa State University

Authors
Omar Smadi, Ahmad Alhasan, and Alireza Sassani

Sponsored by
Iowa Department of Transportation and
Federal Highway Administration
(20-SPR0-008)

Preparation of this report was financed in part
through funds provided by the Iowa Department of Transportation
through its Research Management Agreement with the
Institute for Transportation
(InTrans Project 19-719)

A report from
Center for Transportation Research and Education
Iowa State University
2711 South Loop Drive, Suite 4700
Ames, IA 50010-8664
Phone: 515-294-8103 / Fax: 515-294-0467
https://ctre.iastate.edu

TABLE OF CONTENTS

LIST OF FIGURES

LIST OF TABLES

ACKNOWLEDGMENTS

The research team would like to acknowledge the Iowa Department of Transportation (DOT) for sponsoring this research and the Federal Highway Administration (FHWA) for the state planning and research (SPR) funds used for this project.

EXECUTIVE SUMMARY

Pavement friction significantly contributes to roadway safety by providing the grip required for safe travel. The Iowa Department of Transportation (DOT) has long recognized the importance of evaluating pavement skid resistance and its impact on traffic safety.

Several devices have been developed to measure skid resistance. The Iowa DOT currently uses the locked-wheel skid tester (LWST), which is well accepted across the United States and globally. Due to its relatively narrow speed range and limitations on curves and short, low-speed segments, various types of continuous friction measurement equipment (CFME) have been proposed as alternatives, including the GripTester and sideway-force coefficient routine investigation machine (SCRIM). A broader issue in friction measurement is repeatability and reliability under different operational conditions, with temperature, pavement wetting, and test speed affecting the correlation between different devices.

This study aimed to evaluate candidate CFME technologies for their ability to measure pavement friction at different test speeds and in different operational conditions relative to the LWST currently available at the Iowa DOT. Promising CFME technologies were selected, and a testing program based on statistical procedures was designed to evaluate the devices' suitability for pavement friction evaluation in relation to the friction demand and safety analysis. CFME and LWST testing was performed at three asphalt and three concrete pavement test segments at different speeds and using smooth and ribbed tires, and tests were repeated on different days to determine performance in different operational conditions. A dynamic friction tester (DFT) and laser texture scanner (LTS) were used to verify the correlation between the CFME and LWST and to investigate the impact of pavement texture on dry and wet skid resistance.

The research resulted in guidance and recommendations for friction evaluation on different components of the network, including curves and low-speed segments. These outcomes represent a step toward a consistent procedure for both routine pavement friction evaluation at the network level and spot investigation for high-risk areas.

INTRODUCTION

Background

Besides their devastating impact on roadway users, traffic crashes lead to substantial economic losses at the personal and societal levels. Investigations and studies have shown that traffic crashes are very complex events and can be attributed to several factors, such as road geometry, pavement surface texture and drainage, driver behavior or human factors, traffic operations and safety measures, speed limits, and vehicle functions (Tighe et al. 2000, Jung et al. 2014). Identifying the contributing factors and quantifying their impact on high crash rates at a given pavement section will lead to improved safety planning and more appropriate pavement engineering and maintenance and ultimately will help reduce crashes in a cost-effective manner.

Pavement friction is a significant component that contributes to safety performance by providing the required grip for safe travel. Many studies have pointed out a significant relationship between skid resistance and crash rates under wet and slippery conditions (Hall et al. 2009, de León Izeppi et al. 2016a). However, these correlations can be challenging to derive due to the highly varying and uncontrolled conditions during a crash event and the complex skid resistance mechanism (Henry 2000, Noyce et al. 2005).

Additionally, these correlations are state specific or even site specific in most cases. This variation and the incomplete understanding of the impact of pavement skid resistance on traffic safety can be partly attributed to discrepancies in the procedure to measure and evaluate pavement friction, discrepancies in the procedure to relate friction measurements to friction demand under various operating and weather conditions, a lack of proper procedures relating the measured friction and friction demand to traffic safety, and a lack of a proper definition for friction demand.

To better understand the impact of pavement friction on traffic safety, accurate testing should be performed to estimate the friction characteristics of the pavement surface and the resulting skid resistance. The act of measuring pavement friction, identifying roadway locations with high crash rates related to low skid resistance, and proposing effective friction treatments are all components of a pavement friction management (PFM) program.

Over the past several decades, several devices have been developed in an attempt to accurately measure pavement skid resistance, including the locked-wheel skid tester (LWST), which has been standardized in ASTM E274 since 1965. After reaching the desired test speed, typically 40 mph, water is delivered in front of the test tire, and the braking system is actuated to lock the test tire (Figure 1a). Once the brakes are applied, the tire starts transitioning from a 0% slip ratio, which corresponds to the rolling mode, to a 100% slip ratio, where the tire is fully locked. Force and torque transducers are used to acquire and estimate the tractive forces and vertical loads applied on the tire. These forces are then used to estimate the skid resistance in accordance with ASTM E274. Figure 1b shows a typical screenshot during the locked-wheel test, where it can be noticed that the skid resistance reaches a peak, which typically occurs between a 15% and 30% slip ratio, and drops to a stable value representing the fully locked mode.

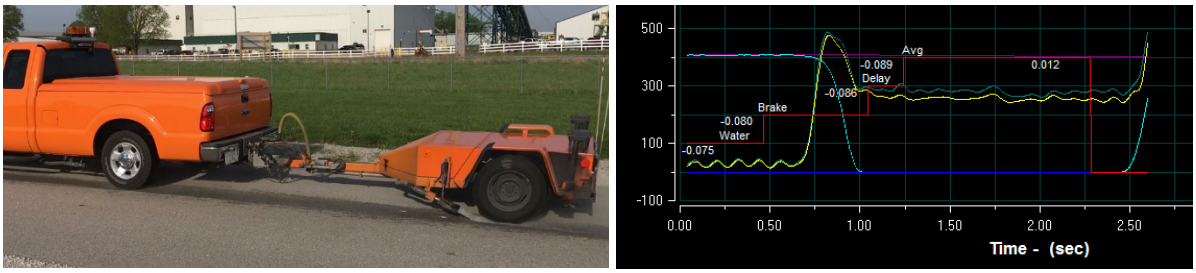

(a) (b)

Figure 1. (a) Locked-wheel test performed in 2017 by the Iowa DOT during a previous study by the research team and (b) screenshot of the test results

The LWST has been continually improved over the years and is currently well accepted across the United States and globally. However, the LWST is only valid at speeds ranging between 40 and 60 mph. In addition, the device has some known limitations when testing on curved and short segments (de León Izeppi et al. 2016b), which represent some of the most critical segments to evaluate for skid resistance. To overcome these limitations, a few types of continuous friction measurement equipment (CFME) have been developed to acquire continuous friction measurements at varying speeds and on tangent or curved segments. Based on the acquired measurements, CFMEs can be classified into longitudinal friction coefficient (LFC) and sideway force coefficient (SFC) devices. Several devices have been developed under both categories; however, the widely accepted devices by the Federal Highway Administration (FHWA) and worldwide are the GripTester, an LFC device, and the sideway-force coefficient routine investigation machine (SCRIM), an SFC device.

The GripTester consists of trailer with a central measuring smooth tire (ASTM E1844) equipped with transducers and sensors to measure the speed and vertical and horizontal forces. This tire is connected to a chain to restrict its rolling movement, which induces a constant slip condition. At this condition, the rolling speed at the tire circumference will be 16% lower than the total tire speed. In such cases, the slippage induces frictional forces between the pavement and tire.

As shown in Figure 2, the measuring wheel in a sideway-force device is rotated at a skew angle to the travel direction, which induces a side friction force in the lateral direction. These forces represent the traction forces that develop when the friction demand exceeds what the road can provide on a curved path (Hall et al. 2009, Flintsch et al. 2012).

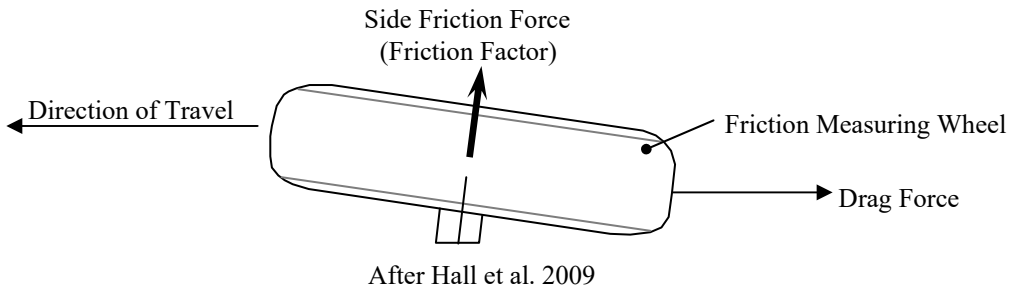

Figure 2. Free-body diagram of a rotating wheel for a vehicle traversing a curved segment

A few sideway-force devices have been developed, including the Mu Meter, the SCRIM, and the RT3 Curve developed by Halliday Technologies. The SCRIM (Figure 3a) was originally developed in the late 1960s by the Transportation Research Laboratory (TRL) in the United Kingdom, and since the 1970s it has been manufactured solely by W.D.M. Limited (TRL 2015a). The machine uses a freely rotating wheel, fitted with a smooth tire angled at 20° to the direction of travel, applied to the road surface under a known vertical load. Similar to the LWST, water is delivered in the front of the measuring wheel so that when the vehicle moves forward, the test wheel slides and the wet skid resistance can be measured at varying speeds. Additionally, the SCRIM can continuously measure friction, cross-slope, macrotexture, grade, temperature, and curvature while being driven up to 50 mph. SCRIM has been widely accepted and deployed in several countries, including the United Kingdom and New Zealand. It is one of the ways FHWA is advancing its PFM Support Program, which aims to reduce highway crashes and fatalities.

More recently, Halliday Technologies (Plain City, Ohio) has produced a promising sideway-force technology, the RT3 Curve, which provides continuous friction measurements at different desired speeds and operating conditions. Figure 3b shows the RT3 Curve trailer, which includes two inner traveling tires and two outside measuring tires, thus providing friction measurement in each wheel path. The outside measuring tires can be fitted with standard ribbed tires (ASTM E501) or smooth tires (ASTM E524), similar to the LWST, and can be angled at a skew angle between 1° and 8°. The system can be operated at varying speeds (between 5 mph and 80 mph) and water flows to meet the recommended 0.02 in. water film thickness (Meyer et al. 1972).

(a) (b)
WDM USA 2019 (left); The Transtec Group 2019 (right)

Figure 3. (a) SCRIM and (b) GripTester curve testing trailer

In summary, the different devices are intended to represent to the actual slippage conditions during a crash event. However, each device captures a part of the more complex and compound behavior during a crash event.

The Iowa Department of Transportation (DOT) has recognized the importance of evaluating pavement skid resistance and its impact on traffic safety since 1965. Moreover, a friction review committee was formed in 1972, which established the pavement friction evaluation program Policy 600.01. The purpose of the policy is “to establish criteria to be used in the evaluation of

frictional characteristics of pavement surfaces and to take action to mitigate low friction coefficient area." The proposed criteria in Policy 600.01 are based on friction number thresholds and assuming that friction impact will be manifested in wet conditions. More recent studies have shown that the impact of friction on traffic safety is more complicated and can interact with various weather conditions. Furthermore, FHWA Technical Advisory T5040.38 states that no single friction value represents the boundary between safe and unsafe pavement surface.

Currently, the Iowa DOT performs friction testing to determine whether the roadway has sufficient available friction to promote safety. The testing cycles are not well defined and are limited due to the limited use of friction data. The Iowa DOT relies on the locked-wheel friction testing method, which has been standardized in ASTM E274 and accepted as a validation of available friction. Despite the widespread use of the locked-wheel skid tester, the application of this method is limited when testing on curves and low-speed roadway segments. This includes high-risk locations such as ramps, intersections, diverging and converging lanes, curves and other low-speed areas.

Problem Statement

With the different devices available to estimate pavement friction, practitioners and researchers have noticed discrepancies in the estimated values. These differences are due to the fact that friction is not a fundamental property of the pavement surface independent of other variables. Friction is a complicated phenomenon that develops due to the interaction between two surfaces under operating conditions that have an impact on this interaction (Meyer et al. 1972). In an early project on this topic, Meyer et al. (1972) conducted an extensive study for the National Cooperative Highway Research Program (NCHRP) to evaluate the repeatability and reliability of the LWST under different operational conditions. It was pointed out that the variables affecting the correlation between different devices can include temperature, pavement wetting, and test speed.

Despite the extensive efforts nationally and worldwide, there is a lack of consistent procedures to evaluate pavement friction and interpret measurements in relation to the friction demand required for safe travel. All previous studies have focused on evaluating friction testing technologies in a controlled testing environment, such as testing facilities and short segments. However, there is less guidance on the consistent use of friction testing at the network level. At the network level, there might be different levels of tolerance in the acceptable measures. Also, there is a lack of procedures to utilize the pavement friction information in safety performance evaluation and, accordingly, a missing link required to establish mature friction management programs. This gap can possibly prevent the Iowa DOT from taking proactive corrective actions that can save lives, money, and resources.

Objectives

The primary objectives of this study were as follows:

- Identify the possible procedures and a list of candidate CFME technologies to evaluate pavement friction at different test speeds and in different operational conditions.
- Assess the feasibility and possible benefits from the list of candidate CFME technologies to be used in Iowa based on their cost, accuracy, and applicability to the intended evaluation outcomes.
- Perform an initial evaluation of the most feasible CFME technologies relative to the LWST currently available at the Iowa DOT.
- Provide guidance and recommend technologies to be used for friction evaluation on different components of the network, including curves and low-speed segments.
- Define a consistent procedure for both routine pavement friction evaluation at the network level and spot investigation for high-risk areas.

Benefits

The results of this study are expected to improve the safety performance and economic and social impacts of Iowa's network. The study produced guidelines and procedures to acquire, analyze, and interpret friction measurements using CFME and LWST. In addition, this research addresses the potential applications and benefits of pavement friction evaluation and the possible development of a mature PFM for the state of Iowa.

Beneficial outcomes for the Iowa DOT, counties, districts, and city engineers include the following:

- Evaluate the feasibility and benefits of CFME in comparison to the available LWST.
- Perform accurate and representative pavement friction evaluation.
- Developing effective pavement friction evaluation plans for routine network testing.
- Evaluate the available skid resistance on high-risk locations, which were not evaluated previously using the LWST.
- Ability to relate pavement friction evaluation to friction demand required for safe travel.
- Facilitate the development of a mature PFM for the state of Iowa.

LITERATURE REVIEW

The team investigated the current practices and available technologies for pavement friction evaluation through an extensive literature review. The review focused on the technologies used to perform friction evaluation on different network segments, efficient procedures for both routine pavement friction evaluation at the network level and spot investigation at high-risk areas, and the interpretability of friction measurements acquired from different devices in relation to friction demand and safety evaluation.

The team also reached out to agencies that have experimented with CFME to help better understand the advantages and limitations of the technology. Recently, Washington, Florida, Indiana, and Texas have demonstrated CFME on their networks, and Ohio has investigated the possible use of CFME. These DOTs were contacted for the task. Additionally, the team coordinated with the FHWA PFM support program to provide guidance and possible support for the project.

Skid Resistance Measurement Devices

A number of devices are used for the characterization of pavement skid resistance, as shown in Table 1. The LWST, SCRIM, GripTester, and pavement friction tester (PFT) are the most commonly used.

Table 1. Skid resistance measurement devices

Method	Description	Standard
LWST	This device is installed on a trailer that is towed behind the measuring vehicle at a typical speed of 40 mph (64 km/h). Water (0.02 in. [0.5 mm] thick) is applied in front of the test tire, the test tire is lowered as necessary, and a braking system is forced to lock the tire. Then the resistive drag force is measured and averaged for 1 to 3 seconds after the test wheel is fully locked. Friction of the pavement surface is determined from the resulting force or torque and is reported as skid number (SN). A higher SN indicates greater frictional resistance. Measurements can be repeated after the wheel reaches a free rolling state again. The LWST can use two different types of tires: ribbed and smooth, as standardized by ASTM E501-94 and ASTM E524-88. Ribbed tire measurements are known to be less sensitive to pavement macrotexture and water film depth than smooth tires. Studies have shown that depending on the type of test tire used, the measurement of skid resistance obtained relates strongly to macrotexture or microtexture. The tire tread of the standard ribbed tire is better for measuring skid resistance relative to macrotexture, whereas the standard smooth tire is better for measuring microtexture-related skid resistance.	ASTM E274

Method	Description	Standard
SCRIM	The SCRIM was originally developed by TRL in England and is one of the most used pieces of equipment in Europe. It uses an oblique wheel system to determine the transversal friction coefficient in terms of a sideway-force coefficient reported as a SCRIM reading (SR). The equipment uses a smooth tire that is mounted at 20° to the direction of travel. A water tank on the vehicle wets the pavement just before the tire, and the test tire has its own weight and suspension. The equipment measures the sideways force and computes sideway-force friction coefficient, which is typically reported as the average for each continuous 10 m section.	ASTM WK40015
GripTester	The GripTester is a braked-wheel, fixed-slip device with drag and load (horizontal and vertical force) continuously monitored and their quotient (coefficient of friction) calculated and displayed (ASTM E2340). It uses a single test wheel equipped with a smooth-tread tire (ASTM E1844) oriented longitudinally to the direction of travel. A chain connected to the axle of the test wheel gives it an approximately 16% fixed-slip ratio so that the test wheel is forced to rotate at a speed slower than that of the drive wheels, thereby generating slip between the test tire and pavement. The test wheel configuration allows the GripTester to measure a longitudinal friction coefficient, referred to as a grip number (GN), at 3 ft (0.914 m) intervals.	BS 7941-2:2000

Although, the ASTM E-274 locked-wheel skid trailer is considered very reliable and repeatable, the method may be less sensitive to changes in friction than other currently available devices and has several limitations, including testing on curves and short roadway segments. Because all friction test methods can be insensitive to macrotexture under specific circumstances, it is also recommended that friction testing be complemented by macrotexture measurement (FHWA 2010). One advantage of CFME over the traditional ASTM E-274 test method is that friction is measured continuously over a test section rather than as an average value over several hundred feet and shows a better relationship to braking with anti-lock brakes (FHWA 2010). The LWST method is meant to test the frictional properties of the surface under emergency braking conditions for a vehicle without anti-lock brakes. Unlike the sideway-force and fixed-slip methods, the locked-wheel approach tests at a slip speed equal to the vehicle speed, which means that the wheel is locked and unable to rotate. The results of the locked-wheel test are reported as a friction number, given as follows:

$$FN(V) = 100 \times \mu = 100 \times (\frac{F}{W})$$

where V = tire velocity, μ = coefficient of friction, F = tractive horizontal force applied to the tire, and W = vertical load applied to the tire.

The SFC in SCRIM is calculated as follows:

$$SFC(V, \propto) = 100 \times \frac{F_S}{W}$$

where V = velocity of the test tire, α = yaw angle, F_S = force perpendicular to the plane of rotation, and W = vertical load applied to the tire.

Fixed-slip devices measure the friction experienced by vehicles with anti-lock brakes. Fixed-slip devices maintain a constant slip, typically between 10% and 20%, as a vertical load is applied to the test tire (Henry 2000). The frictional force in the direction of motion between the tire and pavement is measured, and the percent slip is computed as follows:

$$Percent\ Slip = \frac{(V - r \times \omega)}{V} \times 100$$

where percent slip = ratio of slip speed to test speed, V = test speed, r = effective tire rolling radius, and ω = angular velocity of the test tire.

Skid Resistance Measurement Practices

According to the 2009 TYROSAFE report (Anfosso-Ledee et al. 2009) on skid resistance measurement in the European Union (EU), 4 of the 18 responding EU countries do not have any policy for skid resistance at all, although they have devices for friction measurement. Figure 4 shows the proportion of EU countries in terms of skid resistance measurement.

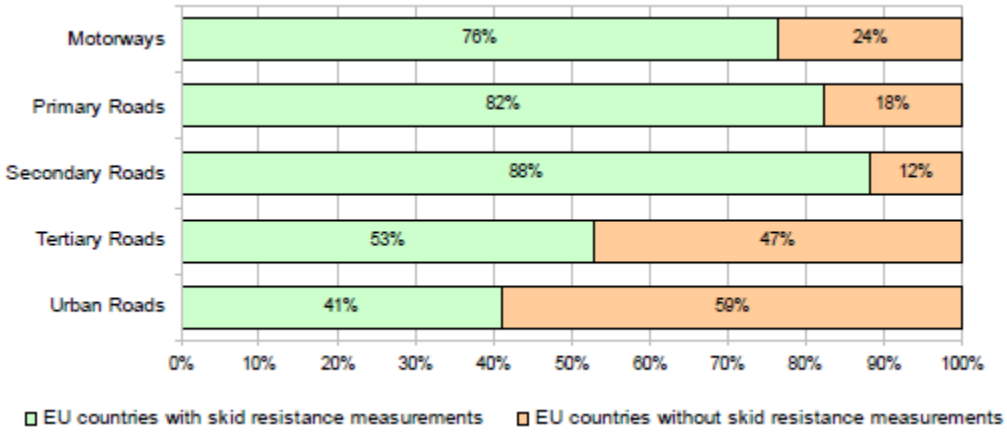

Figure 4. Proportions of EU countries with and without skid resistance measurement

Figure 5 summarizes the numbers of countries using each of the 15 different devices listed to measure skid resistance. The pendulum is the only internationally standardized skid resistance measurement device. Therefore, it features in most skid resistance policies. This is a static device, unsuitable to network monitoring, but it can be used as local complement to the larger mobile dynamic skid resistance measurement devices.

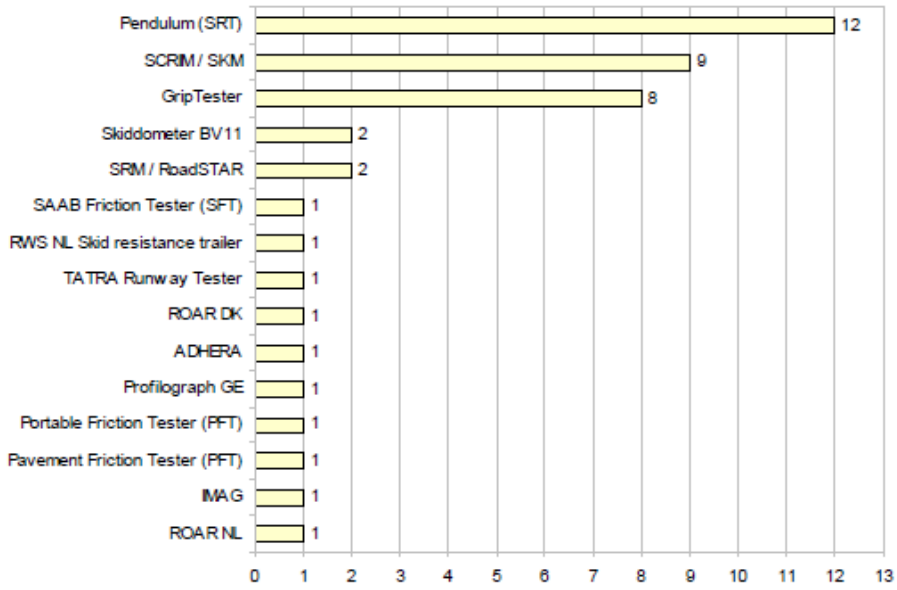

Figure 5. Skid resistance devices and the number of EU countries using them

Figure 6 shows the purpose for which the devices are used in EU countries. Some devices may be used to support the skid resistance standards in that country, whereas others may complement these as a research tool. Fifteen of seventeen EU countries use at least one of their devices for local investigations, and this is the main use for the pendulum tester, again reflecting the common use of the pendulum to complement dynamic devices. SCRIM and GripTester are often applied to local investigations as well. Only ten countries use at least one of their devices to directly support their skid resistance standards.

Device Name	Support skid resistance standard	Part of Condition Index	Local Investi-gations	Research tool	Acceptance tests	Warranty tests
Pendulum (SRT)	1	2	9	7	7	2
SCRIM + SKM	5	3	9	7	7	6
GripTester	1	2	5	6	3	1
Skiddometer BV11	1		2	2	2	2
ADHERA			1	1	1	1
Pavement Friction Tester (PFT)			1	1		
RoadSTAR	1	1	1	1	1	1
ROAR DK + ROAR NL	2		1	2	1	1
RWS NL Skid resistance trailer	1	1	1	1	1	1
SAAB Friction Tester (SFT)			1	1	1	1
Portable Friction Tester (PFT)				1		
Profilograph GE		1				

Figure 6. Skid resistance measurement purpose

Figure 7 and Figure 8 show the extent to which countries carry out routine monitoring on their networks and how often the network is monitored.

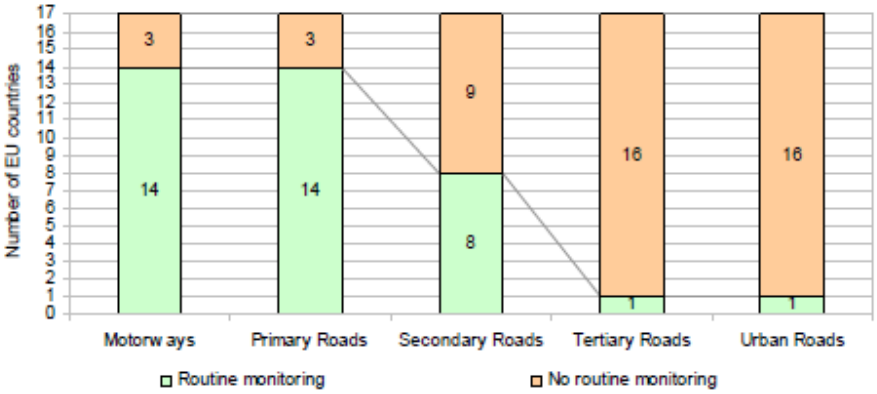

Figure 7. Routine monitoring policies

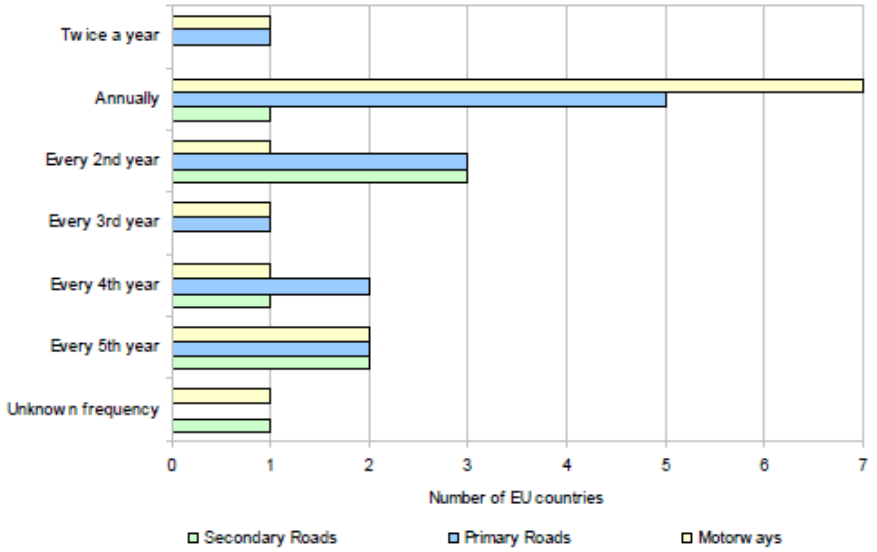

Figure 8. Frequency of routine monitoring

Measurement of Skid Resistance

The skid resistance measurement process is divided into the following six steps:

1. Determine the survey procedure

- The overall (summer) level of skid resistance shall be assessed rather than using a single measurement. This overall level of skid resistance is referred to as the characteristic skid coefficient (CSC).

- The skid resistance of road surfaces can fluctuate within a year and between successive years while maintaining a similar general level over a longer period of time. By smoothing these fluctuations caused by seasonal effects, sites exhibiting lower skid resistance can be identified more accurately.
- The way in which surveys are planned and how seasonal variation is accounted for is provided in the National Application Annexes for each overseeing organization.
- Prior to the survey season, the network to be surveyed, the survey period, the test lane, the survey strategy and the method and/or the accuracy of location referencing required shall be established with the agreement of the overseeing organization.
- Measurements for monitoring the in-service skid resistance of motorway and all-purpose trunk roads shall be made with a sideway-force coefficient routine investigation machine that has been accredited by the overseeing organization for use on its network and not with other skid resistance measurement devices.

2. Plan surveys

- The survey periods shall be defined so that the low point in the summer occurs during the middle period, as shown in Figure 9.

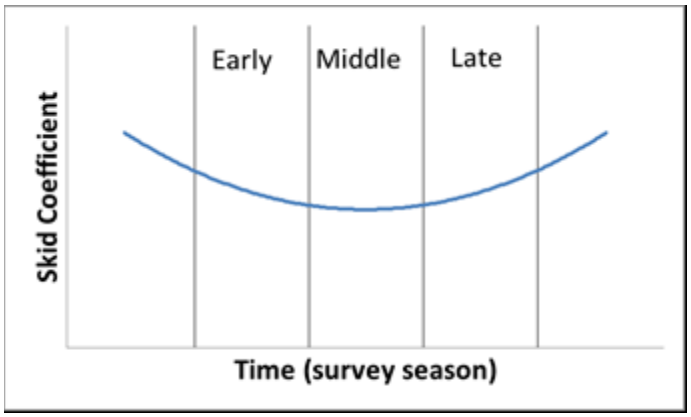

Figure 9. Survey periods

3. Conduct surveys

- The survey contractors shall comply with the calibration and quality assurance detailed in the standard.
- In each direction of travel, the lane carrying the greatest number of heavy vehicles shall be tested. For most roads, this will be the leftmost permanent lane.
- If it is necessary for the machine to deviate from the test line (e.g., to avoid a physical obstruction or surface contamination such as mud, oil, or grit), the data shall be marked as invalid and subsequently discarded. Where it is necessary for the machine to deviate from the test line, the invalid length should be resurveyed at a later date but still within the required survey period.
- Measurements shall not be undertaken where the air temperature is below 5ºC.

- Testing shall be avoided in heavy rainfall or where there is standing water on the road surface.
- Excess water on the surface can affect the drag forces at the tire/road interface and influence the measurements.
- Where the posted speed limit is greater than 50 mph, the target survey speed shall be 80 km/h. On all other roads, the target survey speed shall be 50 km/h (30 mph).
- The machine driver shall maintain a vehicle speed as close to the target survey speed as possible.
- The survey operator shall maintain a record of weather conditions that could influence the survey results, such as heavy rainfall or strong winds.

4. Process survey data

- On completion of the survey, the survey data shall be loaded into the overseeing organization's information management systems and aligned to the road network.
- Readings for each 10 m subsection collected within the speed range 25 to 85 km/h shall be corrected to a speed of 50 km/h.
- Temperature correction shall not be applied.
- Skid coefficient (SC) values shall be calculated for each 10 m subsection for which a valid SR(s) value is available using the following equation:

$$SC = \frac{SR(50)}{100} \times Index\ of\ SFC$$

where the index of SFC is 0.78.

5. Check survey coverage

- The survey machine operator shall produce a survey coverage report detailing the network that was to be surveyed, lengths with missing or invalid data, and an explanation for the missing or invalid data.

6. Apply seasonal correction

- Once the data have been loaded and checked, the seasonally corrected CSC values shall be determined from the SC values following the method appropriate to the survey strategy.

Speed Correction

Test speed has a considerable effect on skid resistance, and therefore most skid resistance standards are written with reference to measurements made at a specific speed. The acceptable range for performing GripTester and SCRIM friction measurements is 15 mph to 55 mph (25 to 85 km/h). The water flow for the GripTester has to be above 2 gal/minute, although it will adapt

dynamically to the speed. The SRs are averaged every 10 m. The GNs are reported every 3 ft. Measurements are then corrected to a standard speed of 30 mph (50 km/h) using the speed correction given in HD28/04. The speed correction can be applied to measurements made between 25 and 85 km/h, which enables variations in speed resulting from traffic levels, road geometry, or traffic control to be accounted for. The adjustment for travel speed corrects GN to 40 mph (64 km/h) and SR to 30 mph (50 km/h), respectively, using the equations below. GN is measured at travel speed (v) and corrected to GN40 using a speed correction factor (SCF) of 0.6/mi. SR is corrected to 30 mph (50 km/h) using the equation specified in the *British Design Manual for Roads and Bridges* (Highways England 2015):

$$GN(40\ mph) = GN(v) + SCF \times (v - 40)$$

$$SR(30\ mph) = \frac{SR(v) \times (-0.0152 \times v^2 + 4.77 \times v + 799)}{1000}$$

where GN (v) and SR (v) are the grip number and skid resistance at speed v

Braking

The effect of braking on skid resistance device readings has been examined. TRL (2015b) collected measurements with SCRIM and GripTester on a test section under braking conditions. The braking section was approached at 25 km/h (15 mph), 50 km/h (30 mph) and 80 km/h (50 mph) and the survey vehicles brought to a stop by deceleration. The figures in this section show how deceleration causes the skid resistance value to differ from the reference. The variation in skid resistance from the reference (reference SR – speed-corrected SR) is shown against the absolute acceleration being experienced at each nominal approach speed. The red horizontal lines represent the range of skid resistance values measured on the reference surface at a constant speed of 50 km/h. Figure 10 shows that the variation in skid resistance measured using SCRIM under braking is greater than that measured at a constant speed and that the range of values measured under braking have a greater range than that of the variation on the reference. Figure 11 shows that the majority of measurements made when braking from 25 km/h are within the variation expected when testing at a constant speed. Measurements made above a deceleration of approximately 2 m/s^2 rapidly move outside of this range, and measurements made at 80 km/h show that the range of the measurement capability of GripTester is being exceeded.

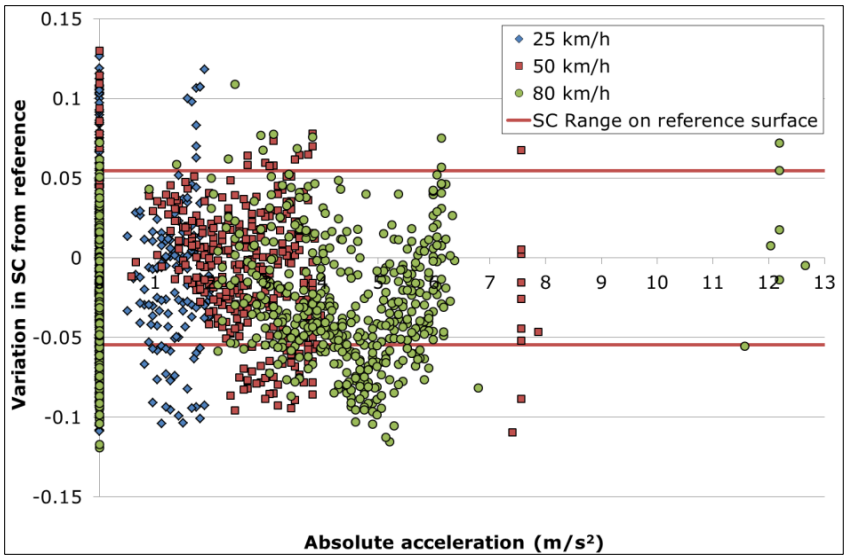

Figure 10. SCRIM variation from reference

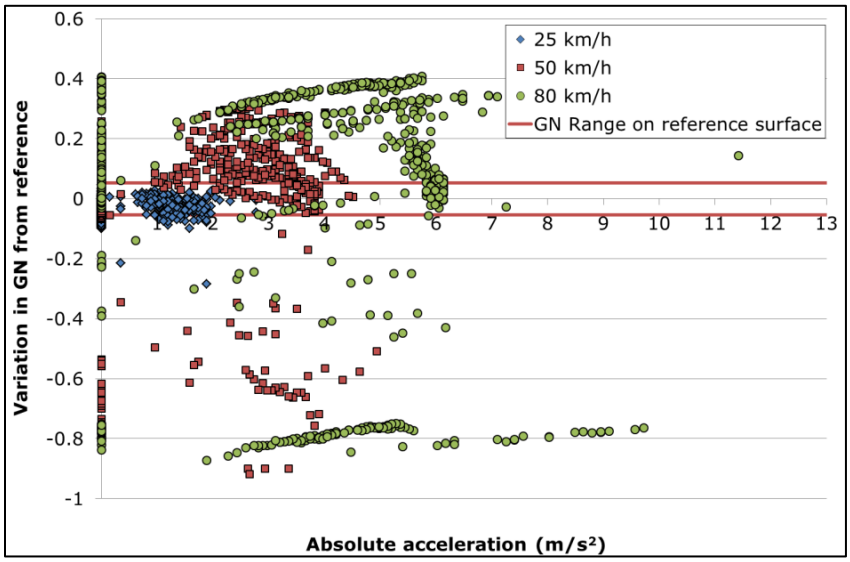

Figure 11. GripTester variation from reference

Dynamic Vertical Load Measurement

BS 7941 states that the mass of the test wheel assembly shall provide a static vertical load of (200 ± 8 kg). Furthermore BS 7941 states that the mass acting on the test wheel should be measured using a load cell. Machines use one of two types of systems, referred to as the "old system" and the "new system." The old system utilizes a sacrificial shear pin that is sensitive to wear, causing it to affect the load measurement. The new system does not use a shear pin and has been found to be more robust and reliable.

Temperature Measurement

There is no requirement for the measurement of temperature in BS 7941. However, if such a requirement is introduced in the European Committee for Standardization (CEN) standard, the fitting of temperature sensors is expected to be straightforward because SCRIM has been designed to allow the addition of this feature if required.

Water Application

BS 7941 stipulates the following for water supply and flow control:

- Water is to be controlled by a manual flow valve that can be adjusted to allow different flow rates depending on test speed.
- The water control system should activate the water flow before the test wheel contacts the ground and should not deactivate until the wheel has left the ground.
- The water shall contact the surface 400 ± 50 mm in front of the center line of the test wheel along the direction of the line of travel.
- The water shall be free from contaminants.
- The theoretical water film thickness shall be 0.5 mm at 50 km/h.

SCRIM can be fitted with a dynamic control system that adjusts the water flow automatically to ensure that the correct flow rate is achieved at a range of test speeds. The essential elements of a dynamically controlled water flow system are a flow meter, proportional control valve, and electronic control system. Either a header water tank or an electric pump is used to ensure that the correct water flow is achievable at high speeds. Dynamically controlled water flow is appealing from an environmental and resource conservation point of view, but there is as yet no evidence to suggest that measurements are markedly improved as a result.

Test Wheel and Tire

BS 7941 specifies using standard test tires for SCRIM that are manufactured by Avon tires and distributed through the equipment manufacturer, which also carries out quality assurance checks. Current standards do not stipulate whether the slip angle of the test tire (20°) should be toe-in or toe-out. SCRIM uses the toe-in position; anecdotally, this seems to have been chosen in the early development of the machine to ensure stability of the vehicle when cornering. In the United Kingdom (UK), skid resistance measurements are normally made in the left wheel track of the most heavily trafficked lane, which is usually the leftmost lane. Due to the UK fleet having the test tire on the nearside of the vehicle (left), these devices are unable to test the nearside wheel track on some European roads, and vice-versa for European machines.

International Friction Index

ASTM E1960, Standard Practice for Calculating International Friction Index of a Pavement Surface, explains how to obtain the International Friction Index (IFI) value from measurements of friction and macrotexture. The IFI consists of two parameters, F60 and S_p. The first value is the friction of the wet pavement at 60 km/h, and the second is the speed number that describes the speed dependence of the friction. The IFI is based on a mathematical model (called the PIARC Friction Model) of the friction coefficient as a function of slip speed and macrotexture. IFI uses reference macrotexture (circular track [CT] meter) and friction (dynamic friction tester [DFT]) measurements to normalize the measurements done with different equipment. It was developed to provide a standard comparison of pavement friction measurements around the world. Through this index, it is possible to compare measurements obtained with different equipment. The IFI speed number and friction number are computed using the following equations:

$$S_p = a + (b \times MPD)$$

where S_p = IFI speed number, a, b = calibration constants depending on method used to measure macrotexture, and a = 14.2 and b = 89.7.

$$FR(60) = FR(S) \times e^{\frac{S-60}{S_p}}$$

where *FR (60)* = friction at the speed of 60 km/h, *FR (S)* = friction value at *S* km/h, and *S* = slip speed.

$$F(60) = A + B \times FR(60) + C \times MPD$$

where *F (60)* = IFI friction number, *A, B* = calibration constants depending on friction measuring device, and *C* = calibration constants required for measurements using a ribbed tire.

Repeatability of SCRIM and GripTester in Literature

Quiros et al. (2018) conducted a study to evaluate interconversion methods between CFME devices and LWST based on the IFI approach. The data collected were used in an analysis of variance (ANOVA) to obtain the variance (or mean squares) needed as the variance factor to calculate the repeatability for each device. The repeatability, r, for each device is calculated using the following equation:

$$r = \sqrt{{s_1}^2} * \sqrt{2} * 1.96$$

where s_1^2 = mean square calculated for the ANOVA analysis for the first group of data.

The repeatability of each device was determined as the limits of agreement (LOA) between the measurements. If the repeatability of a device is low, the agreement between that device and any other will be poor as well. Table 2 shows the repeatability of the three devices computed using the LOA calculated using the above equation. The repeatability seems to be good and similar for all three devices. The table also presents the results from the LOA for pairwise comparisons at the three tested speeds for the three devices studied. The reproducibility between the two LWSTs is good and is close to the repeatability of 14 for each individual device. However, the measurements taken with both LWSTs are ±10 units approximately to the SCRIM measurements with a 95% level of confidence at the three speeds. This suggests that the measurements are different. This was expected because the two devices are measuring different frictional properties at very different slipping speeds. Although the testing speed is the same for the three devices, the actual slipping speed for the SCRIM is lower (by approximately one-third) than that of the LWST. These results reinforce the need for speed corrections.

Table 2. Repeatability computed using LOA

Equipment	Speed	Repeatability
TTI LWST	30	1.4
	40	1.3
	50	3.5
TxDOT LWST	30	1.1
	40	2.5
	50	4.5
SCRIM	30	3.3
	40	2.9
	50	1.3

In TRL Published Project Report PPR771 (TRL 2015b), the standard for SCRIM accreditation was used based on the Pavement Condition Information Systems guidelines (PCIS 2013), which stipulate that the between-equipment standard deviation threshold for the SCRIM fleet is 2.7 SR. It was deemed prudent that this value also be used for the performance threshold for the reference surfaces.

TRL Published Project Report PPR497 (TRL 2010) discusses skid resistance data collected from 11 GripTesters. Skid resistance was measured by all machines, each having its own dedicated tow vehicle and crew, on sections of the TRL track and on sections of local in-service roads. In addition, two SCRIM machines were used to measure skid resistance on the same surfaces. Figure 12 shows the average grip number measured by each GripTester. The values highlighted in bold and italics are those measurements that fall more than two measurements outside of the mean, with 8% of values more than two standard deviations from the mean. No values fall more than three standard deviations from the mean.

Section	GripTester										
	A	B	C	D	E	F	G	H	J	K	L
1	0.46	0.47	0.49	0.57	0.50	0.47	0.47	***0.63***	0.54	0.55	0.55
2a	0.38	0.41	0.43	0.46	0.46	0.44	0.41	***0.57***	0.46	0.50	0.45
2b	0.76	0.79	0.79	0.81	0.90	0.75	0.79	***1.02***	0.87	0.91	0.83
3	0.60	0.61	0.60	0.65	0.62	***0.53***	0.59	0.66	0.67	0.67	0.68
4	0.62	0.62	0.61	0.65	0.64	0.55	0.61	0.70	0.68	0.70	0.67
5a	0.74	0.74	0.72	0.76	0.81	***0.66***	0.74	0.81	0.83	0.79	0.81
5b	0.42	0.44	0.45	0.48	0.49	0.45	0.43	***0.60***	0.46	0.50	0.48
6	0.45	0.46	0.48	0.48	0.46	***0.39***	0.46	0.50	0.49	0.53	0.51
7a	0.48	0.50	0.51	0.52	0.51	***0.42***	0.51	0.52	0.58	0.54	0.54
7b	0.62	0.68	0.63	0.66	0.63	***0.54***	0.65	0.66	0.70	0.71	0.71
8	0.45	0.48	0.49	0.48	0.49	***0.41***	0.46	0.50	0.54	0.53	0.52

Figure 12. Average grip number measured by each GripTester

Figure 13 shows the average skid resistance measured by all GripTesters on the road sections, pooled between run standard deviation (s_r), repeatability (r), pooled between machine standard deviation (s_L), and reproducibility (R). The average repeatability for the GripTester fleet was found to be 0.10 GN, and the average reproducibility for the GripTester fleet was found to be 0.17 GN.

	Section	Mean	s_r	r	s_L	R
Road sections	1	0.52	0.05	0.14	0.05	0.21
	2a	0.45	0.04	0.11	0.05	0.18
	2b	0.84	0.05	0.14	0.08	0.26
	3	0.63	0.05	0.13	0.05	0.18
	4	0.64	0.04	0.11	0.05	0.17
	5a	0.76	0.05	0.14	0.05	0.20
	5b	0.47	0.03	0.08	0.05	0.16
	6	0.47	0.02	0.06	0.04	0.12
	7a	0.51	0.03	0.09	0.04	0.14
	7b	0.65	0.03	0.08	0.05	0.16
	8	0.49	0.03	0.08	0.04	0.13

Figure 13. Average skid resistance measured by all GripTesters

Figure 14 shows the SCRIM measurements on the same sections as the GripTester measurements. The repeatability of the SCRIM was calculated as 0.03 SC.

	Section	SCRIM		Mean SC	Mean GN
		X	Y		
Road sections	1	0.48	0.51	0.49	0.52
	2a	0.45	0.44	0.44	0.45
	2b	0.67	0.71	0.69	0.84
	3	0.55	0.54	0.55	0.63
	4	0.53	0.54	0.53	0.64
	5a	0.70	0.66	0.68	0.76
	5b	0.43	0.44	0.43	0.47
	6	0.45	0.43	0.44	0.47
	7a	0.47	0.47	0.47	0.51
	7b	0.58	0.53	0.55	0.65
	8	0.46	0.44	0.45	0.49

Figure 14. SCRIM measurements on the same sections as the GripTester measurements

Roe and Sinhal (2005) discussed issues relating to the calibration and comparison of skid resistance measurements from the perspective of the UK experience of using SCRIM machines to collect skid resistance data and applying acceptance criteria. The following were the criteria regarding repeatability of SCRIM machines:

- The between-run standard deviation on any individual section for any individual machine and tire should be 3.0 or less.
- The maximum standard deviation between the overall machine means is 2.6.
- Any machine that is 7.8 or more (i.e., three times a standard deviation of 2.6) from the all-machine mean will be rejected outright.
- Any machine that is between 5.2 and 7.8 (i.e., between two and three times a standard deviation of 2.6) from the mean will be subject to further investigation in the context of the overall distribution and performance on the full range of surfacings.

TESTING PROGRAM

The team contacted technology and service providers, including W.D.M. Limited and Halliday Technologies, and inquired about cost estimates for purchasing the equipment or services and about showcase studies at the national and international levels. The search covered LFC and SFC devices such as the GripTester and the SCRIM. The feasibility of each technology was evaluated based on the technology's cost, benefits, ease of use, versatility, and availability.

Once the technologies were selected, the team designed a testing program to evaluate their suitability for pavement friction evaluation in relation to the friction demand and safety analysis. The testing plan was designed based on statistical procedures to cover the possible testing variables of interest, including the following:

- Surface type
- Surface age
- Traffic volume
- Road geometry
- Prevailing traffic speed

Furthermore, the experimental design accounted for the testing required to correlate the new CFME results to the results acquired using the standard LWST available at the Iowa DOT. The intent of these correlations was not to derive global harmonization procedures and friction models but rather to allow for interchangeability between the testing procedures, facilitating smooth future implementation and possible transition to and adoption of the new technologies.

Site Selection

Test segments were selected in coordination with the Iowa DOT. The testing program included six control sites to assess and contrast the different friction devices included in the study. Three asphalt cement concrete (AC) and three portland cement concrete (PCC) surfaces were selected, as shown in Table 3.

Table 3. Selected control sites

Site	Location	Route	Surface
1	Perry	IA 141	PCC
2	Jefferson	IA 4	AC
3	Indianola	IA 92	PCC
4	Bondurant	US 65	PCC
5	Boone	US 30	AC
6	Ogden	US 30	AC

Since one of the major advantages of the SCRIM is the collection of continuous data on long stretches of the highway network, including tangent and curved segments, in this study the

SCRIM was used to acquire additional data on 15 curves, including 4 high-friction surface treatments (HFSTs), and 4 tangent validation segments, as shown in Table 4, to assess network-level data collection. The curves were selected to include various surface types, radii of curvature, and surface treatment ages to assess the usability of the devices under different conditions, as shown in Table 4. The data on the curves and miscellaneous segments were acquired at prevailing traffic speeds. However, the speed was relatively consistent within each test section.

Table 4. Selected curves

Site ID	Route	Surface Type	Radius (ft)	Age (Years)
C1	IA 14	AC	< 500	> 10
C2	IA 150	JPCP	> 1500	> 10
C3	US 30	Microsurfacing	500 to 1000	> 10
C4	IA 281	Seal Coat	500 to 1000	> 10
C5	US 52	AC	< 500	< 2
C6	IA 13	JPCP	> 1500	< 2
C7	US 63	AC	500 - 1000	5 - 10
C8	IA 130	AC	< 500	2 - 5
C9	IA 210	AC	500 - 1000	2 - 5
C10	IA 330	AC	500 - 1000	< 2
C11	US 218	AC	500 - 1000	> 10
HFST1	IA 5	HFST	> 1000	> 10
HFST2	IA 137	HFST	> 1000	> 10
HFST3	White Pole Rd	HFST	500 - 1000	> 10
HFST4	Summit Rd	HFST	< 500	> 10
Val 1	IA 4	Varying	-	-
Val 2	US 30	Varying	-	-
Val 3	US 65	Varying	-	-
Val 4	IA 141	Varying	-	-

Texture and Friction Measurement

The CFME service providers performed CFME testing on the selected segments. The CFME tests were matched with LWST tests at selected locations. The LWST tests were performed by the Iowa DOT following the standard procedure outlined in ASTM E274 at 30, 40, and 50 mph. Ribbed and smooth tires were used to acquire the ribbed and smooth skid numbers. The tests were repeated three times at each test speed, and each location was visited twice to detect variability between the results from day to day, which can be affected by the devices' operational conditions.

In addition to friction testing at highway speeds, the DFT and laser texture scanner (LTS) were used to verify the correlation between the CFME and LWST in accordance with ASTM E1960. Moreover, surface texture scans were conducted to investigate the impact of pavement texture on dry and wet skid resistance.

Overall, the friction measurement devices included the LWST, SCRIM, DFT, and the British pendulum tester (BPT). In addition to the friction testing, surface texture was acquired using a high-density stationary texture scanner and the high-speed texture profiler attached to the SCRIM. Figure 15 outlines the tests performed at the control sites.

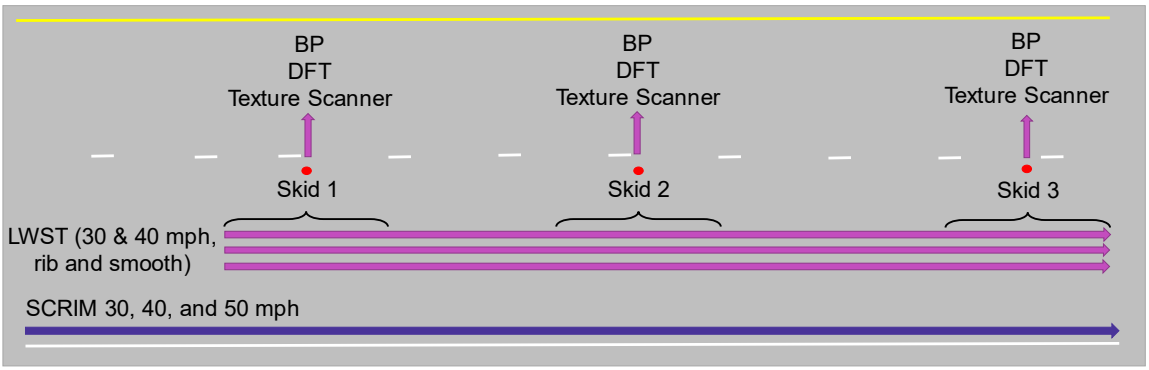

Figure 15. Field tests performed at control sites

Dynamic Friction Tester (DFT)

Dynamic friction tests were performed at the same spots where the BPT and stationary laser texture scans were acquired. The tests were performed in accordance with ASTM E 1911. The standard test procedure is performed on a wet surface. However, the first test spot at site 4 was performed on a dry surface, and therefore its results were not included in the analysis set. The test starts with surface wetting, which is supplied to the device by an attached water tank. During the surface wetting, the disk shown in Figure 16b spins until the rubber pads reach the target circumferential speed. The measurement speed can range between 6.2 and 49.7 mph (i.e., 10 and 80 km/h). After reaching the target speed, the spinning disk is lowered and pressed against the road surface due to the device weight. The friction developing between the road surface and the three rubber pads induces resisting torque, which slows down the spinning disk. The frictional forces estimated from the measured torque is then divided by the normal force on the pads due to the device weight to estimate the coefficient of friction (COF) at different speeds as the disk slows down. All data acquisition and speed are controlled with a laptop connected to the device. The DFT readings were taken at all control sites as shown in Figure 15.

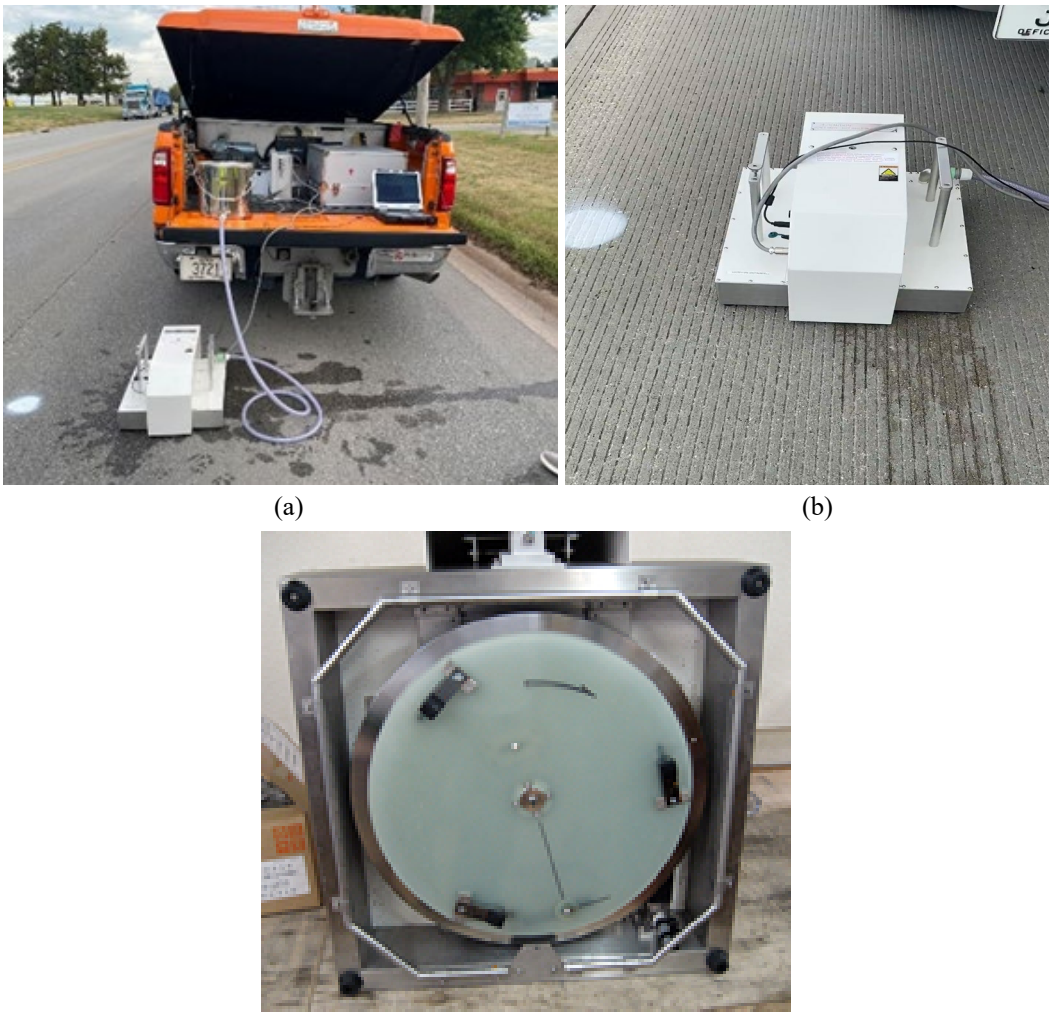

(a) (b)

(c)

Nippo Sangyo Co., Ltd.

Figure 16. DFT device: (a) side view, (b) close-up view, and (c) rotating disk with three rubber sliders

British Pendulum Tester

Wet British pendulum tests were performed in accordance with ASTM E303 at three tests points, corresponding to the texture measurements, at all the control sites. At each test point, five repeated measurements were acquired, and the last four readings were used to estimate the average British pendulum number ($\overline{BPN}$) and the measurement standard deviation. Figure 17 shows the British pendulum tester, which consists of a pendulum rotating about a spindle attached to a vertical pillar. At the end of the tubular arm, a head of known mass is fitted with a rubber slider 2.99 × 0.98 × 0.24 in. The pendulum is released from a horizontal position so that it strikes the sample surface at an approximate constant velocity of 6.2 mph and a contact pressure of approximately 30 psi. The contact path travelled by the head after striking the surface is between 4.88 and 5 in. Since tire-pavement friction is speed dependent, the test captures the low-speed friction characteristics of the pavement surface, which is typically related to pavement

microtexture. However, several studies have pointed out the significant correlation between BPT results and macrotexture characteristics.

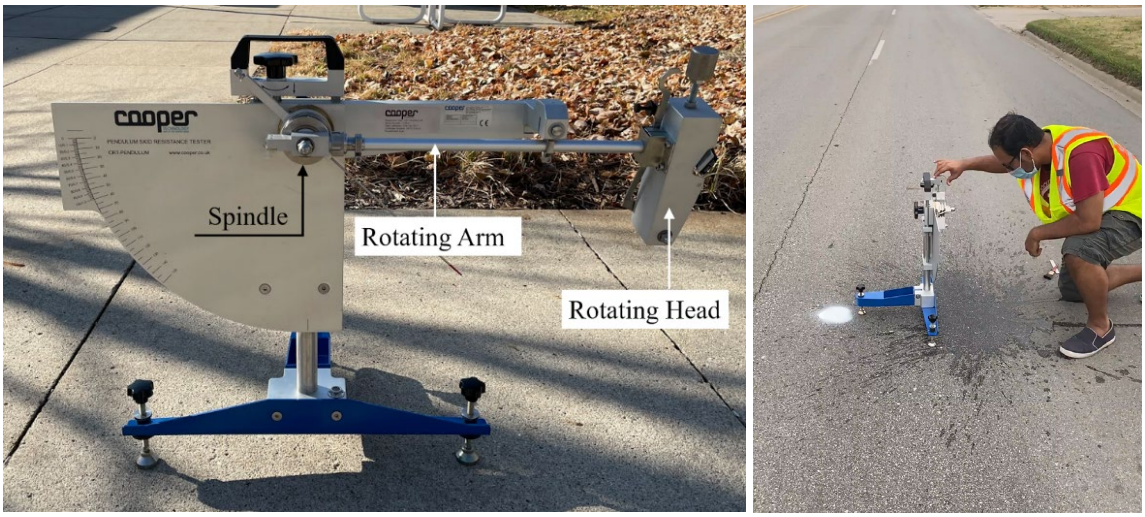

(a) (b)

Figure 17. British pendulum tester: (a) close-up view and (b) in operation

Texture Scanner

Texture measurements were acquired using the high-density stationary LTS at three spots (as outlined in Figure 15) at all control sites in accordance with ASTM E1845. The data from site number 5 (in Boone, Iowa) were acquired. However, the files were corrupt and could not be used for further analysis. Surface texture scans were acquired using the LTS model 9400HD from Ames Engineering. Using LTS 9400HD, the scanned area for all test points was 68.45 × 100.00 mm (2.70 × 3.94 in.), as shown in Figure 18. The scanner acquires single point measurements along 100 line scans with a spacing between the points within each line of 6.35×10^{-3} mm (0.25×10^{-3} in) and a total length of 100 mm (3.94 in.). The spacing between the line scans was set to 0.69 mm (2.7×10^{-2} in). This allows the capture of macrotexture and a part of the microtexture of the scanned area in the longitudinal direction. The scanner uses a red laser with a dot size of 25×10^{-3} mm at the center of range, with a 22° triangulation angle at the center of range. The acquired points are then processed in a triangulation analysis algorithm to produce a 3D point cloud of the surface texture.

Figure 18. Stationary LTS

Locked-Wheel Skid Tester (LWST)

The locked-wheel skid test was performed at the six control sites in accordance with ASTM E274 using the ribbed tire (ASTM E501) and smooth tire (ASTM E524) at 30 and 40 mph, as shown in Figure 19. Three skids were acquired in each test run with the stationary test points within the skid span, as shown in Figure 15. The tests were repeated three times, resulting in a total of 36 runs with 108 skids. The test device records the tractive force, defined as the horizontal force applied to the test tire at the tire-pavement contact patch, and the dynamic vertical load on the test wheel. The ratio of tractive force to the vertical load multiplied by 100 defines the skid number at a given testing condition, including the test speed. During the test, the trailer wheels are locked after applying water (0.5 mm thick) to the test surface. Ribbed tire measurements are known to be less sensitive to pavement macrotexture and water film depth than smooth tires. Studies have shown that depending on the type of test tire used, the measurement of skid resistance obtained will relate strongly to macrotexture or microtexture. The tire tread of the standard ribbed tire is better for measuring skid resistance relative to macrotexture, whereas the standard smooth tire is better for measuring microtexture related skid resistance.

(a) (b)

Figure 19. Locked-wheel skid tester: (a) close-up view and (b) in operation

Sideway-Force Coefficient Routine Investigation Machine (SCRIM)

The SCRIM is equipment originally developed by TRL in the United Kingdom and is predominantly used in Europe. It uses an oblique wheel system to determine the transversal

friction coefficient in terms of a sideway-force coefficient reported as a SCRIM reading. The equipment uses a smooth tire that is mounted at 20º to the direction of travel. A water tank on the vehicle wets the pavement just before the tire, and the test tire has its own weight and suspension. The equipment measures the sideways force and computes a sideway-force friction coefficient, which is typically reported as the average for each continuous 10 m section.

In this study, the SCRIM, shown in Figure 20a, was used to acquire data at 4 of the control sites (Site 1 – Perry, Site 2 – Jefferson, Site 4 – Bondurant and Site 6 – Ogden) and at 15 curves and 4 miscellaneous tangent segments of the Iowa network. The tests on control sites were performed at 30, 40, and 50 mph, which can capture the effect of speed on the measurements. The length of the test stretch on the control sites was 0.62 mi (1000 m), with a 32.81 ft (10 m) reporting interval. During the test, the measuring tire shown in Figure 20b acquires continuous friction measurements, reported as SRs, and macrotexture profiles characterized using the mean profile depth (MPD). The frictional forces developing on the measuring tire develop due to the slip angle from the travel direction, as shown in the schematic in Figure 20c. No break forces are applied to the measuring tire; therefore, the friction mechanism is different from the friction mechanism developing in a LWST. This difference in the friction mechanism results in different measured values since friction is not an intrinsic property of the pavement surface and is affected by the tire material, tire geometry, tire slip ratio, slip angle, and speed, among other variables.

(a)
WDM USA

(b)
WDM USA

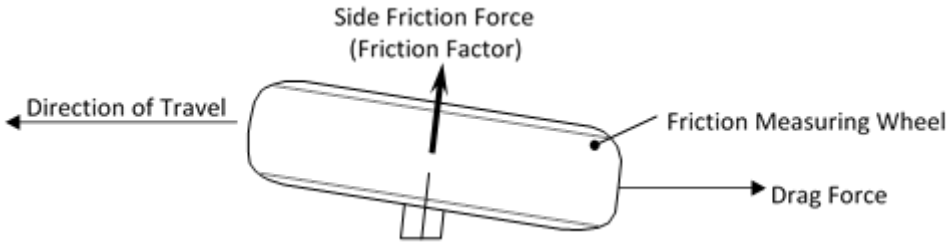

(c)
After Hall et al. 2009

Figure 20. (a) SCRIM equipment, (b) the measuring tire (after), and (c) free-body diagram of the measuring tire

To account for the difference in the friction measurements acquired at different speeds, the following equation is recommended by the manufacturer and previous studies to shift the measurements of SR(v) acquired at a speed v to a standard measurement of SR30 acquired at a speed of 30 mph. It should be mentioned that speed in the equation calculations is in km/h units and that the actual recorded speed, not the nominal test speeds, should be used.

$$SR30 = SR(v)\ \frac{(-0.015v^2 + 4.765v + 799.25)}{1000}$$

ANALYSIS AND RESULTS

Based on the measurements acquired during friction testing, the analysis focused on three major aspects:

- **Measurement repeatability**. Several sources of uncertainty can impact the repeatability of LWST and CFME measurements. The team perform uncertainty analysis to quantify the level of repeatability in the acquired measurements. Repeatability was analyzed for each device, at different test speeds, and on different surfaces.
- **Measurement consistency**. Previous studies have indicated the spatial variability in skid resistance across a uniform segment (Meyer et al. 1972), which can impact the repeatability of LWST and CFME measurements and the conclusions drawn based on repeated measurements. The spatial variability on the selected test segments was characterized using the acquired DFT and texture measurements. Although the measurements were expected to differ between the devices, the variation trends were expected to be closely related and to provide a good estimate of the device consistency. In addition, the variations across different pavement surface with different friction measurements (estimated using the DFT and LWST) were expected to be properly captured using the CFME
- **Interpretability and interchangeability**. According to the standard procedure described in ASTM E1960, friction measurements vary as a function of speed and slip angle/ratio. Figure 21 summarizes the procedure outlined in ASTM E1960 to convert and harmonize friction measurements acquired from different devices.

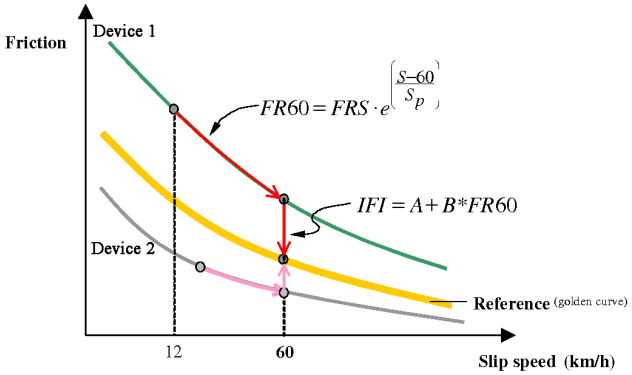

Wallman and Astrom 2001

Figure 21. Demonstration of the IFI

This behavior plays a significant role in evaluating the provided pavement skid resistance in comparison to the friction demand, which is a function of speed among other variables. The data acquired at different speeds were evaluated to test their suitability and interpretability for friction-speed models. Additionally, correlations were derived to relate the friction-speed curves acquired using the LWST and CFME.

The following subsections present a descriptive analysis and basic correlation analysis of the acquired friction and texture measurements.

Texture Measurements

Several roughness parameters are calculated in the LTS software tool provided by the manufacturer, including the MPD and estimated texture depth (ETD) in accordance with ASTM E1845, average roughness (R_a), root mean square roughness (R_q), skewness (R_{sk}), and kurtosis (R_{ku}). All of the mentioned parameters are calculated for the individual lines within the scan and then averaged to represent the overall roughness parameter of the scanned area. Table 5 provides a summary of the averaged roughness parameters for the five control sites.

Table 5. Summary of roughness parameters estimated using stationary LTS

Site	Point	MPD	ETD	R_a	R_q	R_{sk}	R_{ku}
1	1	1.05E-02	1.64E-02	5.18E-03	6.91E-03	-1.12	2.27
	2	1.16E-02	1.72E-02	6.09E-03	8.29E-03	-1.18	2.23
	3	1.08E-02	1.66E-02	5.16E-03	7.09E-03	-1.02	2.50
2	1	1.19E-02	1.76E-02	6.86E-03	9.56E-03	-1.50	5.16
	2	9.56E-03	1.57E-02	5.25E-03	7.49E-03	-1.51	4.91
	3	9.34E-03	1.55E-02	5.16E-03	7.54E-03	-1.80	5.98
3	1	1.50E-02	2.00E-02	9.60E-03	1.31E-02	-1.52	3.12
	2	1.59E-02	2.07E-02	1.16E-02	1.59E-02	-1.52	2.44
	3	2.14E-02	2.51E-02	1.78E-02	2.27E-02	-1.38	1.17
4	1	1.66E-02	2.13E-02	9.78E-03	1.29E-02	-1.04	2.34
	2	1.25E-02	1.80E-02	8.02E-03	1.06E-02	-0.71	1.88
	3	1.46E-02	1.97E-02	9.18E-03	1.15E-02	-0.60	0.78
6	1	2.10E-02	2.48E-02	8.61E-03	1.12E-02	-0.39	0.90
	2	2.01E-02	2.40E-02	9.35E-03	1.23E-02	-0.66	1.13
	3	2.27E-02	2.62E-02	1.05E-02	1.35E-02	-0.47	0.75

Although the number of measured points is limited for robust quantitative conclusions, Figure 22 indicates that the roughness parameters show collinearity, which has an impact when using these parameters simultaneously in multiple linear/nonlinear regression models to describe pavement friction. The equations relating the roughness parameters on the y-axis (y variable) and the MPD on the x-axis (x variable) and the coefficients of determination (R^2) provided in the figures are derived based on the limited data set in this study and therefore should be considered as a descriptive summary and not general correlations for a wide range of applications. It should be mentioned that the scatter plot between MPD and ETD is not included Figure 22 because ETD was estimated based on the correlation provided in ASTM E1845 (ETD = 0.008 + 0.8 MPD), and therefore the scatter plot will not provide additional information. Figure 22a and Figure 22b show that the scatter plots of MPD versus R_a and R_q have similar trends and the strongest positive correlation. Figure 22c shows a negative correlation between the MPD and kurtosis (R_{ku}). Generally, surfaces with kurtosis values less than 3 tend to have narrower peaks (spiky surfaces), and surfaces with kurtosis values greater than 3 tend to have a bumpy surfaces and

more rounded peaks, while surfaces with kurtosis values close to or equal to 3 are referred to as Gaussian surfaces. Figure 22d and Table 5 indicates that all sites are negatively skewed.

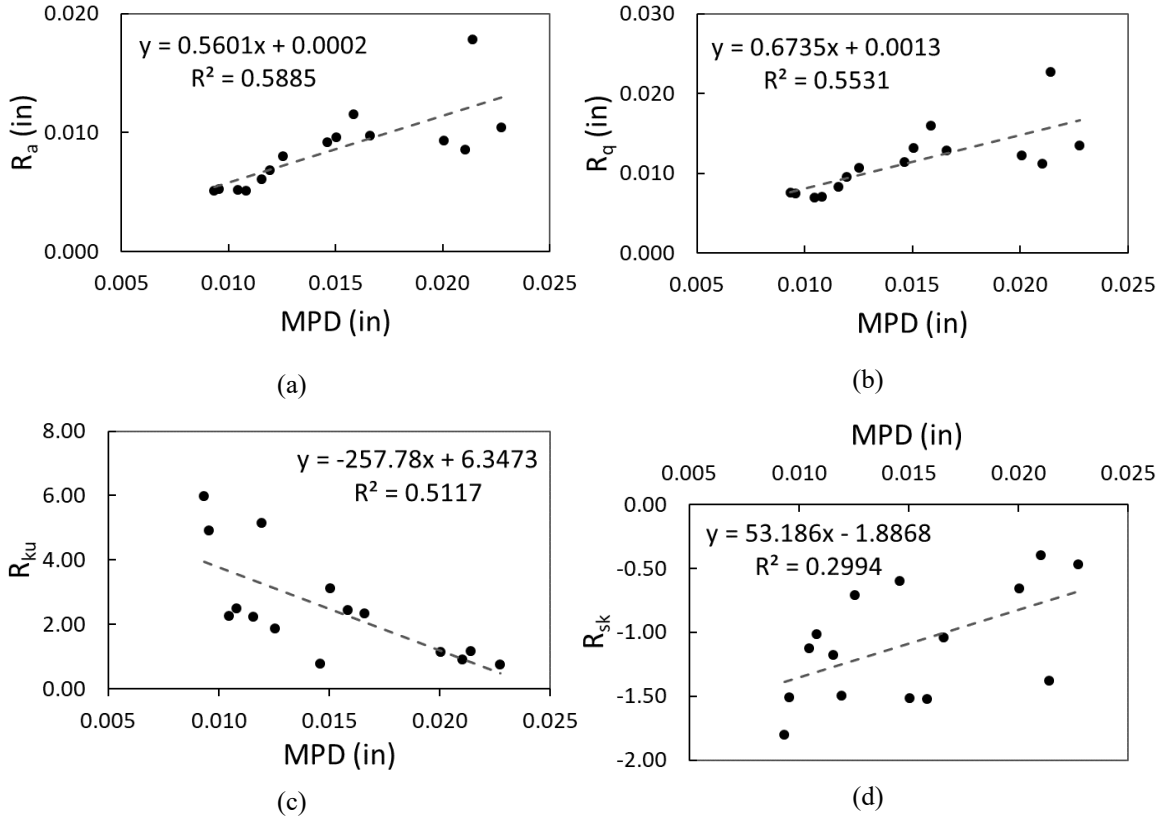

Figure 22. Correlation of MPD to other surface texture parameters estimated from the scans acquired using the stationary LTS

As depicted in Figure 23, negatively skewed surfaces have narrower valleys and wider asperities, which can provide a greater contact area between the pavement surface and the tire. Alternatively, positively skewed surfaces have narrower asperities, which may induce more hysteresis deformations of the tire. Despite the sparse literature on the topic, there is no conclusive evidence of how these two types of surfaces would affect the tire-pavement friction and skid resistance.

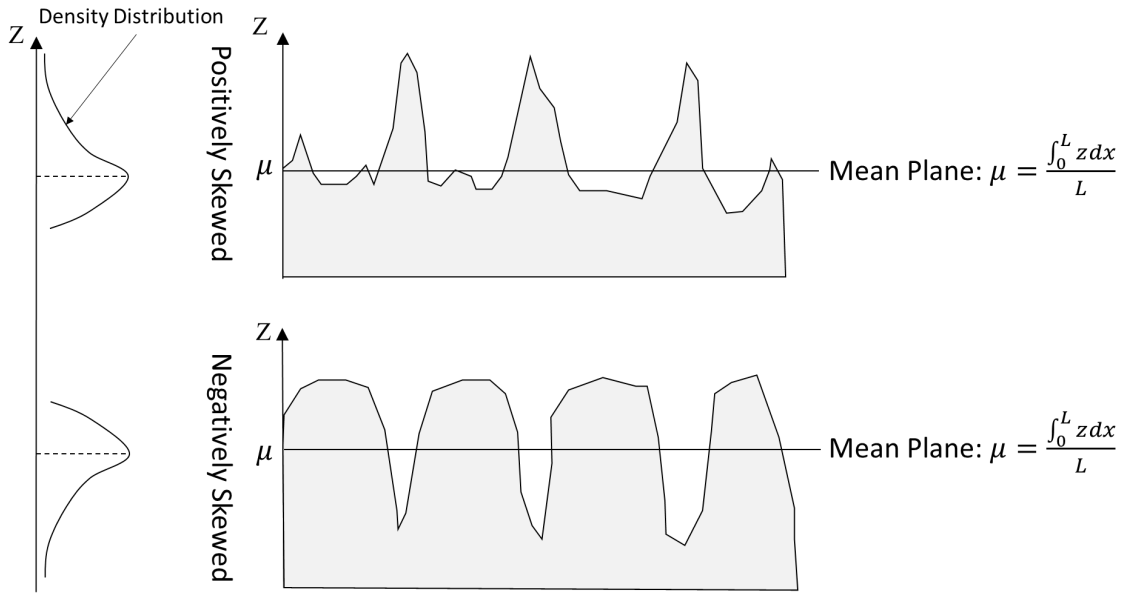

Figure 23. Schematic showing typical texture profile of positively and negatively skewed surfaces

In addition to the texture measurements acquired using the stationary LTS, the SCRIM acquired texture profiles during the friction testing. These profiles are then processed to produce a discrete set of MPD measurements averaged and reported every 10 m. The SCRIM testing was performed for sites 1, 2, 4, and 6 at 3 speeds of 30, 40, and 50 mph. Figure 24 presents the measured MPD acquired from the control sites at three different test speeds. Ideally, the mean profile depth should not change when acquiring data at different speeds. However, there are some differences between the MPD profiles acquired at different speeds. Typically, the sample cross-correlation is used to quantify the degree of agreement between the profiles acquired at different speeds. The Pearson product-moment correlation coefficient (r_{ijl}) shown in the following equation is used in this study as the sample normalized cross-correlation estimator, where $r_{ijl} = 0$ indicates no agreement between the two profiles and $r_{ijl} = 1$ indicates an exact match between the two profiles.

$$r_{ijl} = \frac{\sum_d (MPD_{ild} - \overline{MPD_i})\left(MPD_{jld} - \overline{MPD_j}\right)}{\sqrt{\sum_d (MPD_{ild} - \overline{MPD_i})^2 \sum_d \left(MPD_{jld} - \overline{MPD_j}\right)^2}}$$

where i is the number of the first profile, j is the number of the second profile, l is the lag between two profiles, d is the distance along the profile, MPD_{ild} is the MPD at a given distance d in profile i at a given lag l, and $\overline{MPD_i}$ is the average MPD of a given profile i.

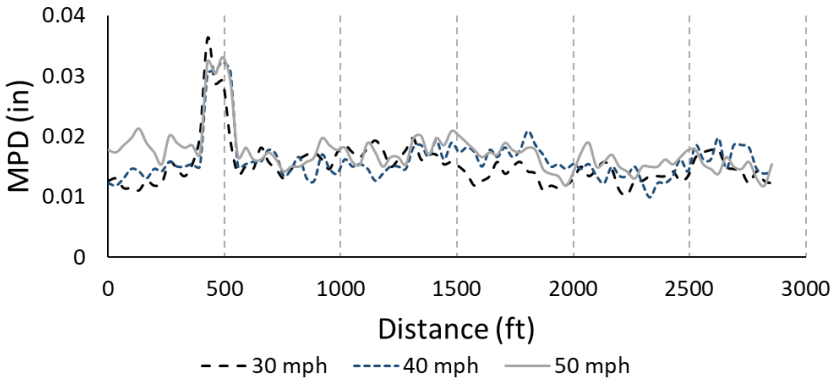

(a) Site 1

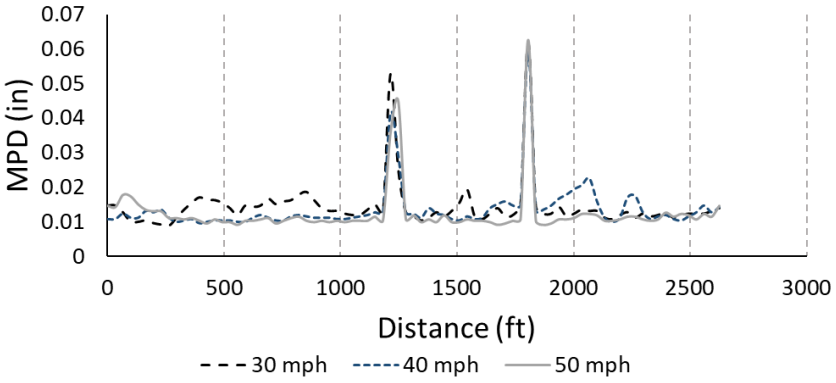

(b) Site 2

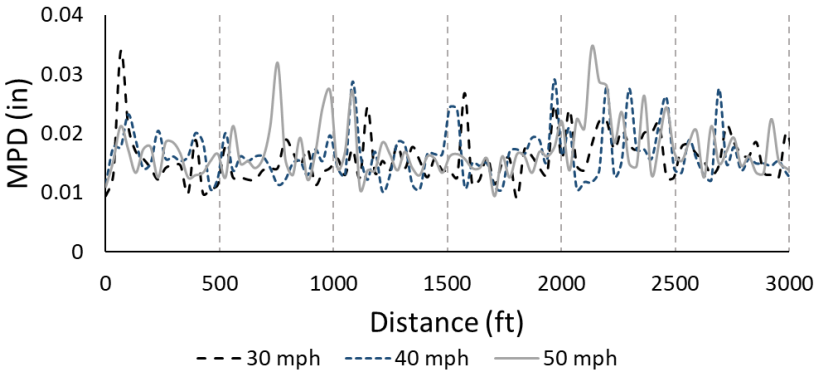

(c) Site 4

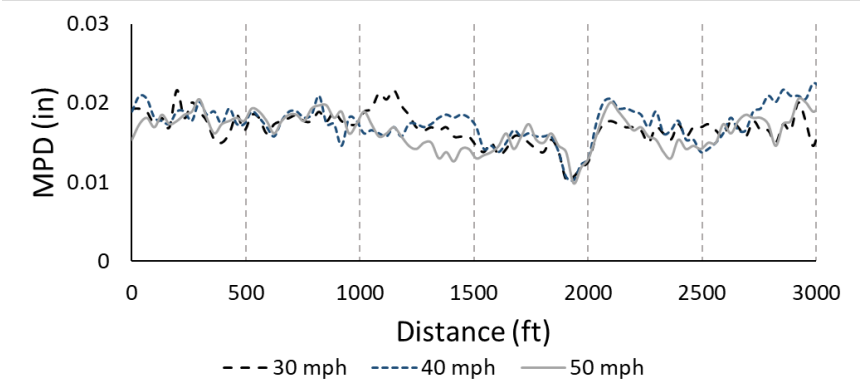

(d) Site 6

Figure 24. Profiles showing the MPD acquired using the SCRIM operated at 30, 40, and 50 mph at control sites (a) 1, (b) 2, (c) 4, and (d) 6

Table 6 presents the maximum cross-correlation values between the profiles across the different sites. It should be noted that some profiles had to be lagged to obtain the maximum cross-correlation value. The cross-correlation values ranged from 0.12 to 0.89.

Table 6. Summary of cross-correlation between the MPD profiles acquired using the SCRIM operated at 30, 40, and 50 mph

Site	Equipment Speed (mph) – Profile *i*	Equipment Speed (mph) – Profile *j*	Correction Lag (32.8 ft/lag)	Cross-Correlation
1	30	40	-1	0.74
	30	50	0	0.71
	40	50	0	0.79
2	30	40	0	0.86
	30	50	0	0.84
	40	50	0	0.89
4	30	40	0	0.20
	30	50	2	0.27
	40	50	1	0.12
6	30	40	0	0.54
	30	50	0	0.60
	40	50	0	0.64

In this study, the average of the MPD values acquired using the SCRIM at the closest point to the stationary LTS, the point before it, and the point after it was used to compare the MPD values estimated using the SCRIM and the stationary LTS. Table 7 presents the spatially matched MPD values acquired at speeds of 30, 40, and 50 mph and the MPD values acquired using the stationary LTS. Figure 25 presents the scatter plot of the MPD values acquired with the stationary LTS and the MPD acquired using the SCRIM at the three test speeds. The fitted regression lines and the corresponding correlations represented in the following equations show that there is a linear correlation between the MPD acquired using the LTS and SCRIM.

$$MPD_{30} = 0.84\ MPD_{LTS} + 0.002,\ R^2 = 0.43$$

$$MPD_{40} = 0.58\ MPD_{LTS} + 0.007,\ R_2 = 0.63$$

$$MPD_{50} = 0.33\ MPD_{LTS} + 0.012,\ R^2 = 0.25$$

Table 7. Summary of MPD measurements acquired using the SCRIM operated at 30, 40, and 50 mph and the stationary LTS

		SCRIM			LTS
Site	**Point**	**MPD30 (in)**	**MPD40 (in)**	**MPD50 (in)**	**MPD (in)**
1	1	1.13E-02	1.39E-02	1.99E-02	1.05E-02
	2	1.46E-02	1.51E-02	1.85E-02	1.16E-02
	3	1.60E-02	1.56E-02	1.68E-02	1.08E-02
2	1	1.23E-02	1.14E-02	1.67E-02	1.19E-02
	2	9.58E-03	1.04E-02	1.09E-02	9.56E-03
	3	1.64E-02	1.01E-02	9.97E-03	9.34E-03
4	1	2.27E-02	1.96E-02	1.80E-02	1.66E-02
	2	1.36E-02	1.75E-02	1.65E-02	1.25E-02
	3	1.31E-02	1.64E-02	1.51E-02	1.46E-02
6	1	1.85E-02	1.98E-02	1.75E-02	2.10E-02
	2	1.90E-02	1.89E-02	1.93E-02	2.01E-02
	3	1.78E-02	1.78E-02	1.84E-02	2.27E-02

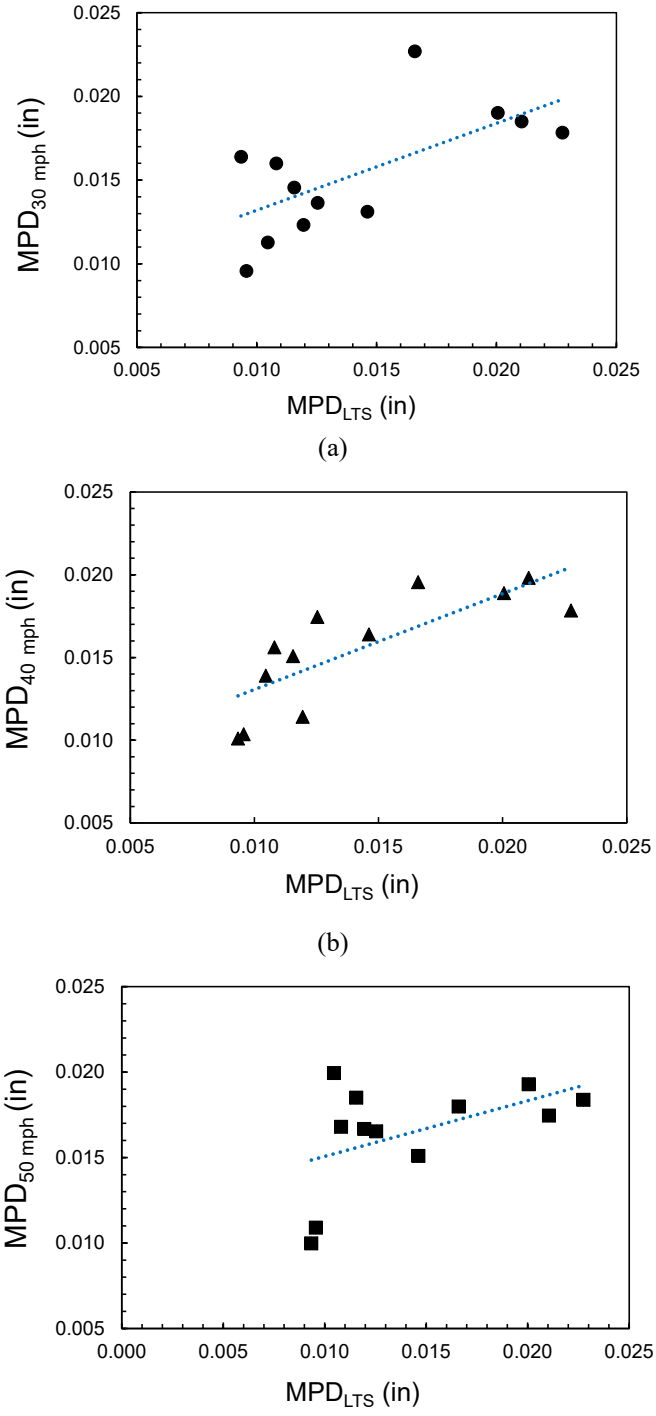

Figure 25. Scatter plots with fitted linear regression lines of the MPD acquired using the SCRIM versus the MPD acquired using the stationary LTS: (a) SCRIM operated at 30 mph, (b) SCRIM operated at 40 mph, and (c) SCRIM operated at 50 mph

Friction Measurements

This section presents the descriptive analysis of friction measurements acquired on the control sites using the SCRIM, LWST, DFT, and BPT. The friction measurements are analyzed for individual devices and related to the texture measurements in separate subsections. Additionally, the measurements acquired using different devices are compared and contrasted.

British Pendulum Test (BPT)

Table 8 presents the summary of British pendulum measurements paired with the MPD acquired using the stationary LTS and the SCRIM operated at 40 mph. It can be noticed that the standard deviation of the measurements is equal to or less than 1 BPN unit, except for two test points. The tested surfaces had a relatively wide range of BPN values. Figure 26a presents the average BPN versus the MPD acquired using the LTS. There is a clear linear positive trend; however, a limited number of observations and pavement surface types limits the ability to derive general conclusions applicable to a wide range of surfaces. Figure 26b presents the average BPN versus the MPD acquired using the SCRIM test at 40 mph, which is more scattered ($R^2 = 0.19$) compared to the trend when using the MPD acquired using the LTS ($R^2 = 0.63$). Trends between the average BPN and MPD acquired using the SCRIM at other speeds had higher scatter and resulted in a weaker correlation with BPN.

Table 8. Summary of British pendulum tests

Site	Point	$\overline{BPN}$	σ_{BPN}	MPD (in)	MPD_{40} (in)
1	1	42.8	0.50	1.05E-02	1.39E-02
	2	43.5	0.58	1.16E-02	1.51E-02
	3	40.5	0.58	1.08E-02	1.56E-02
2	1	54.5	0.58	1.19E-02	1.14E-02
	2	53.5	0.58	9.56E-03	1.04E-02
	3	52.5	0.58	9.34E-03	1.01E-02
3	1	63.0	0.00	1.50E-02	N/A
	2	65.0	1.15	1.59E-02	N/A
	3	57.5	0.58	2.14E-02	N/A
4	1	49.5	1.00	1.66E-02	1.96E-02
	2	49.5	1.29	1.25E-02	1.75E-02
	3	45.8	0.50	1.46E-02	1.64E-02
5	1	44.5	0.58	N/A	N/A
	2	45.5	1.00	N/A	N/A
	3	42.0	0.00	N/A	N/A
6	1	79.8	0.50	2.10E-02	1.98E-02
	2	77.3	0.96	2.01E-02	1.89E-02
	3	85.3	0.50	2.27E-02	1.78E-02

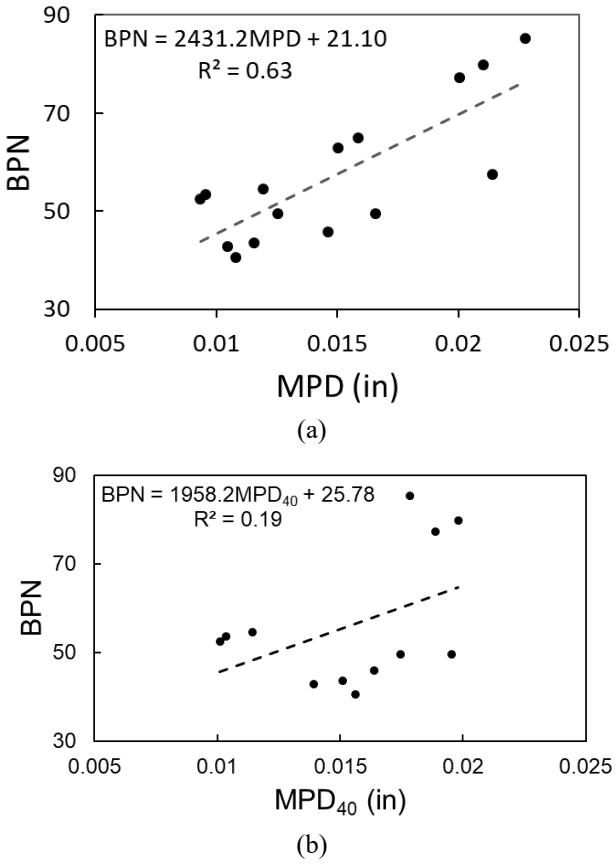

Figure 26. Average BPN versus the MPD estimated using the (a) stationary LTS and (b) SCRIM operated at 30 mph

Dynamic Friction Tester (DFT)

Figure 27 shows two acquired COFs plotted against speed at spots at sites 1 and 3. From the figure, it can be noticed that the COF generally decays at a relatively low rate as the speed increases, until reaching a speed closer to 50 mph, after which COF drops significantly. The curve shape and magnitude can vary significantly from one location to another. This is due to the change in the surface texture and the constituting components of the road surface, which alters both the hysteresis and adhesion components of friction. It should be noted that the geometry of the rubber sliders and the fact that they have a sliding mechanism different from the full tire tests yields measurements different from those of the LWST and the SCRIM. These factors affect the friction mechanism and, accordingly, the friction coefficients acquired from these different devices. To compare the DFT results with those of the other devices, there are four speeds of interest: 6.2 mph corresponding to BPT, 30 and 40 mph corresponding to the LWST and the SCRIM equipment speed, and 50 mph corresponding to the maximum speed of the SCRIM equipment. It should be noted that the SCRIM tire is not locked during the test, and therefore the speeds only correspond to the testing equipment speed and a relative sliding speed between the tire and pavement. Additionally, the readings at the maximum (49.7 mph) and minimum (6.2 mph) DFT speeds seem highly variable; therefore, only the COFs at speeds of 30 and 40 mph were used for further analysis

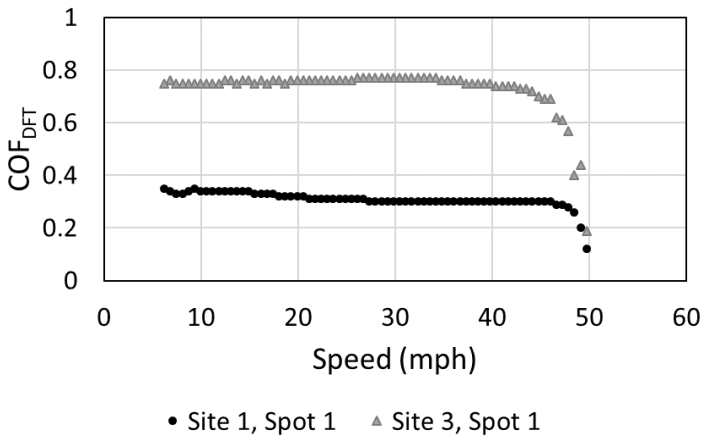

Figure 27. Typical COF versus speed acquired using the DFT

Table 9 presents the summary of COF acquired using the DFT at 30 and 40 mph paired with the MPD acquired using the stationary LTS and the SCRIM operated at 40 mph. It can be noticed that there is no significant difference between the COFs at 30 and 40 mph. Figure 28 presents the COFs acquired by the DFT at 30 and 40 mph versus the MPD acquired using the LTS, which had a linear positive trend. Figure 29 presents the COFs acquired by the DFT at 30 and 40 mph versus the MPD acquired using the SCRIM at 40 mph, which had R^2 values similar to those obtained from correlating the COF to the MPD acquired using the LTS.

Table 9. Estimated COFs using the DFT at 30 and 40 mph coupled with the MPD measurements acquired using the stationary LTS and SCRIM operated at 40 mph

Site	Point	COF_{DFT30}	COF_{DFT40}	MPD (in)	MPD_{40} (in)
1	1	0.30	0.30	1.05E-02	1.39E-02
	2	0.32	0.30	1.16E-02	1.51E-02
	3	0.32	0.31	1.08E-02	1.56E-02
2	1	0.31	0.32	1.19E-02	1.14E-02
	2	0.31	0.31	9.56E-03	1.04E-02
	3	0.32	0.32	9.34E-03	1.01E-02
3	1	0.77	0.75	1.50E-02	N/A
	2	0.51	0.52	1.59E-02	N/A
	3	0.49	0.49	2.14E-02	N/A
4	1	N/A	N/A	1.66E-02	1.96E-02
	2	0.41	0.39	1.25E-02	1.75E-02
	3	0.43	0.42	1.46E-02	1.64E-02
5	1	0.25	0.26	N/A	N/A
	2	0.26	0.28	N/A	N/A
	3	0.25	0.26	N/A	N/A
6	1	0.66	0.66	2.10E-02	1.98E-02
	2	0.68	0.68	2.01E-02	1.89E-02
	3	0.67	0.67	2.27E-02	1.78E-02

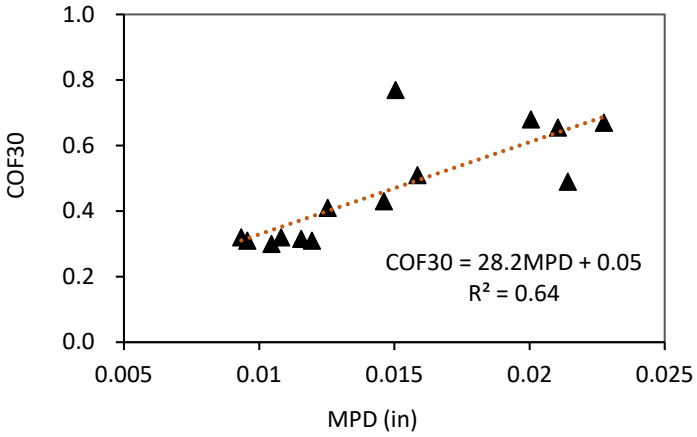

(a)

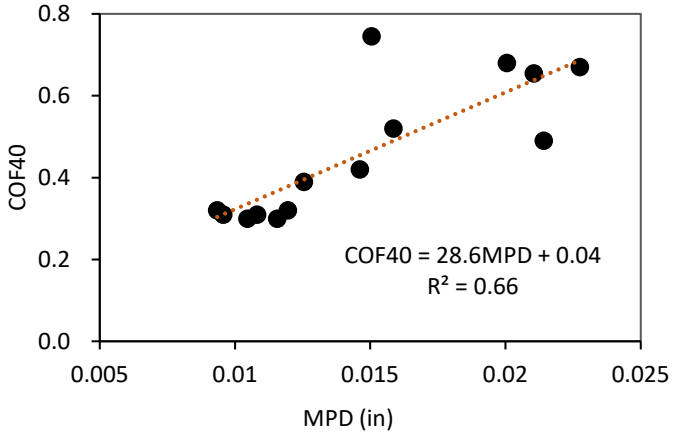

(b)

Figure 28. COFs acquired using the DFT versus the MPD acquired using the stationary LTS: (a) COF at 30 mph, (b) COF at 40 mph

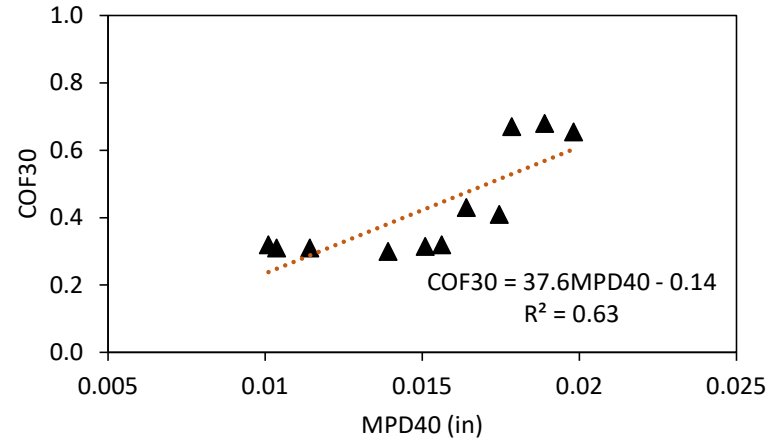

(a)

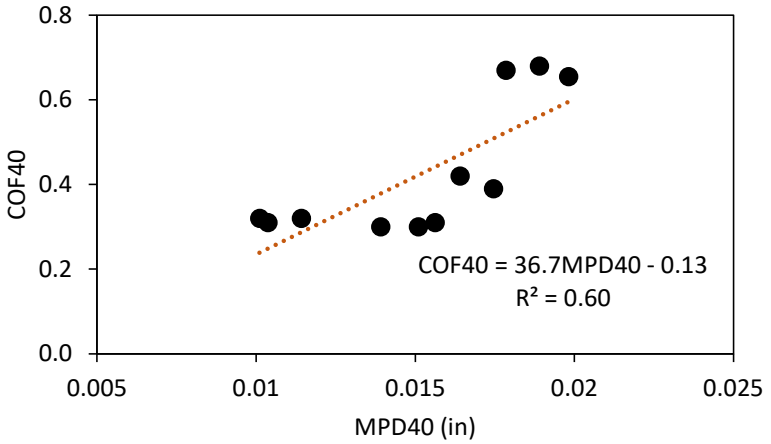

(b)

Figure 29. COFs acquired using the DFT versus the MPD acquired using the SCRIM operated at 40 mph: (a) COF at 30 mph, (b) COF at 40 mph

Locked-Wheel Skid Tester (LWST)

Figure 30 presents a typical screenshot of the locked-wheel test output. In the figure, it can be seen that the SN (the yellow line in the figure) fluctuates around zero, when the tire rotates over the pavement surface without sliding. Then, as the rolling speed decreases and the sliding speed increases accordingly, the SN increases to reach a peak value before dropping back to a fully locked SN, where the rolling speed reaches zero. The fully locked span covers between 1 and 1.5 seconds, which corresponds to 44.0 to 66.0 ft when the test is run at 30 mph and 58.7 to 88.0 ft when the test is run at 40 mph. The summary report from the test includes the peak skid number (SN_{Peak}), the average skid number ($SN_{Average}$) of the fully locked skid numbers of each skid, and the spatial coordinates of the start and end point of the skid.

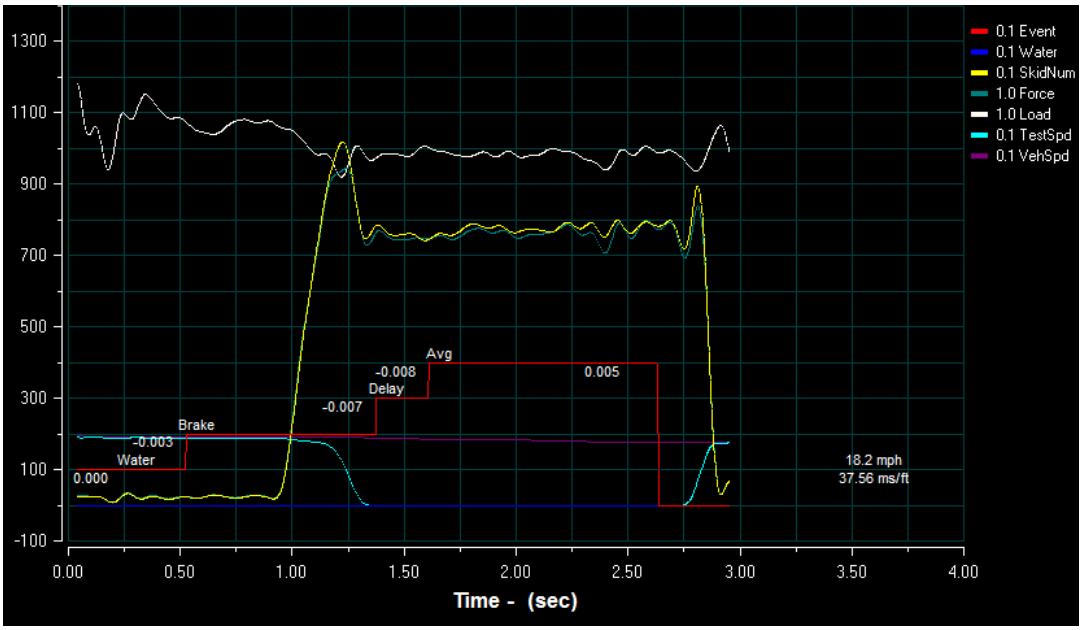

Figure 30. Typical LWST measurements displayed during the test

Table 10 and Table 11 present the average and standard deviation values of SN_{Peak} and $SN_{Average}$ from the three repeated runs with both smooth and ribbed tires at all sites for tests run at 30 mph and 40 mph. Since the measurements with different conditions were acquired over the same point, paired t-tests were performed to test the statistical significance at a 95% confidence level of the difference between the peak and average SNs, the SNs acquired using smooth and ribbed tires, and the SNs acquired at 30 and 40 mph. Obviously, the peak SNs are significantly higher than average SNs acquired using smooth and ribbed tires at 30 and 40 mph. Additionally, the peak and average SN values acquired using the ribbed tire are significantly higher than the values acquired using the smooth tire at 30 and 40 mph. Finally, the peak and average SN values acquired using the smooth and ribbed tires at 30 mph were higher than the values acquired at 40 mph.

Table 10. Summary of LWST results for tests performed at 30 mph

Site	Point	Smooth Tire				Ribbed Tire				MPD (in)	MPD_{40} (in)
		$\overline{SN_{Peak}}$	$\sigma_{SN_{Peak}}$	$\overline{SN_{Average}}$	$\sigma_{SN_{Average}}$	$\overline{SN_{Peak}}$	$\sigma_{SN_{Peak}}$	$\overline{SN_{Average}}$	$\sigma_{SN_{Average}}$		
1	1	38.83	3.06	21.33	0.74	66.07	0.80	37.40	0.87	1.05E-02	1.39E-02
	2	35.43	1.10	18.83	0.61	61.63	5.32	35.87	0.46	1.16E-02	1.51E-02
	3	31.93	1.10	20.27	0.49	60.43	1.72	37.57	0.65	1.08E-02	1.56E-02
2	1	45.83	2.27	21.40	0.82	71.73	1.63	40.80	0.61	1.19E-02	1.14E-02
	2	39.23	1.55	21.30	1.04	66.90	4.10	40.33	1.54	9.56E-03	1.04E-02
	3	41.20	2.20	21.87	0.91	66.43	2.97	38.60	0.72	9.34E-03	1.01E-02
3	1	49.25	1.84	31.63	2.49	86.70	3.90	50.53	1.93	1.50E-02	N/A
	2	57.13	3.59	37.15	1.69	84.00	2.19	55.90	0.89	1.59E-02	N/A
	3	57.08	2.27	43.58	1.67	78.10	0.42	57.30	0.85	2.14E-02	N/A
4	1	74.63	1.60	45.30	0.95	85.73	2.39	52.30	1.68	1.66E-02	1.96E-02
	2	63.70	2.57	44.50	0.44	78.77	2.25	52.03	1.29	1.25E-02	1.75E-02
	3	66.73	1.40	44.10	0.56	76.40	3.52	51.40	1.06	1.46E-02	1.64E-02
5	1	47.03	1.68	25.30	1.56	67.87	2.72	34.20	0.44	N/A	N/A
	2	43.30	1.67	25.93	1.63	60.37	2.20	34.37	0.91	N/A	N/A
	3	45.07	1.21	27.83	1.65	62.67	0.55	36.70	1.15	N/A	N/A
6	1	74.77	2.03	47.40	0.36	105.37	0.64	75.07	0.60	2.10E-02	1.98E-02
	2	73.83	3.70	50.60	1.14	101.27	1.17	74.13	1.42	2.01E-02	1.89E-02
	3	71.57	2.81	49.20	0.56	97.87	1.71	73.13	1.24	2.27E-02	1.78E-02

Table 11. Summary of LWST results for tests performed at 40 mph

Site	Point	Smooth Tire				Ribbed Tire				MPD (in)	MPD_{40} (in)
		$\overline{SN_{Peak}}$	$\sigma_{SN_{Peak}}$	$\overline{SN_{Average}}$	$\sigma_{SN_{Average}}$	$\overline{SN_{Peak}}$	$\sigma_{SN_{Peak}}$	$\overline{SN_{Average}}$	$\sigma_{SN_{Average}}$		
1	1	29.90	0.62	15.60	0.61	62.70	0.79	29.93	0.68	1.05E-02	1.39E-02
	2	26.30	0.30	14.20	0.70	52.97	1.10	31.57	0.40	1.16E-02	1.51E-02
	3	24.87	0.70	15.93	0.60	55.60	3.03	31.73	0.40	1.08E-02	1.56E-02
2	1	30.47	1.50	14.63	0.42	67.58	2.21	35.30	0.77	1.19E-02	1.14E-02
	2	25.53	0.81	14.60	0.17	61.08	2.35	35.13	1.37	9.56E-03	1.04E-02
	3	24.93	1.86	14.63	0.60	54.07	2.74	35.70	0.70	9.34E-03	1.01E-02
3	1	40.27	3.37	22.50	2.50	86.07	3.72	46.73	1.55	1.50E-02	N/A
	2	47.37	4.25	29.83	1.75	77.03	3.84	51.03	1.00	1.59E-02	N/A
	3	50.27	6.37	38.00	3.24	74.60	6.78	51.97	1.27	2.14E-02	N/A
4	1	67.33	2.12	36.20	0.40	77.80	4.96	44.40	0.46	1.66E-02	1.96E-02
	2	51.57	1.24	34.67	0.06	74.87	2.02	45.57	0.96	1.25E-02	1.75E-02
	3	49.20	2.21	32.20	0.17	70.43	1.32	45.30	1.57	1.46E-02	1.64E-02
5	1	35.17	1.43	18.17	0.29	64.13	4.71	30.63	1.07	N/A	N/A
	2	30.83	1.12	18.17	0.55	57.70	3.55	31.33	0.78	N/A	N/A
	3	31.83	0.47	20.53	0.35	57.20	0.82	31.67	0.74	N/A	N/A
6	1	68.87	7.30	41.00	3.56	101.77	0.74	66.87	1.10	2.10E-02	1.98E-02
	2	68.87	3.81	44.63	4.05	100.97	1.19	67.93	0.31	2.01E-02	1.89E-02
	3	64.33	4.86	42.27	3.84	98.50	1.37	66.03	0.75	2.27E-02	1.78E-02

It was not intended to perform a full-scale repeatability and reproducibility evaluation of the LWST in this study. However, the results of a simple regression analysis are reported in this section to estimate the correlation between the corresponding points from repeated LWST runs at all control sites. It should be noted that the since all data sets in the regression models are random, it is more appropriate to develop a random regression model. However, the typical linear regression model with a deterministic regressor was used due to the limited data and since the analysis is descriptive.

The linear regression model summarized in Table 12 has the form $SN_{Run1} = \beta_0 + \beta_1 SN_{Run2,3}$. Table 12 shows that the correlation and coefficient of determination are significantly high. More importantly, the intercept coefficients have very small values and are statistically insignificant (except for the average SN acquired using the ribbed tire at 30 mph) with a p-value greater than 0.05 at a 95% confidence level. The insignificance of the intercept regression coefficients and slope coefficients close to 1.0 indicate that there is no significant bias between the repeated runs. Moreover, it can be noted that there is more variability (i.e., lower R^2) in the correlation for the peak SN values. Although the repeated runs cover the same stretch of road, there can be some shift in the spatial location of the measured points across different runs. The variability in the spatial location of the repeated measurements can contribute to the variability across the repeated runs. This effect can be more pronounced with peak SN value, since they are more sensitive to the surface condition.

Table 12. Linear regression between repeated LWST data

Test Condition	Regressor (x-variable)	Regressand (y-variable)	Parameter	P-value	Correlation Coefficient	R^2 (%)
Ribbed, 30 mph	$SN_{Av.}$, Run1	$SN_{Av.}$, Run2	$\beta_0 = 2.53$	0.03	0.996	99.27
			$\beta_1 = 0.95$	<0.05		
	$SN_{Av.}$, Run1	$SN_{Av.}$, Run3	$\beta_0 = 1.61$	0.27	0.993	98.70
			$\beta_1 = 0.97$	<0.05		
	$SN_{Peak.}$, Run1	$SN_{Peak.}$, Run2	$\beta_0 = 3.13$	0.40	0.982	96.39
			$\beta_1 = 0.96$	<0.05		
	$SN_{Peak.}$, Run1	$SN_{Peak.}$, Run3	$\beta_0 = 2.78$	0.66	0.951	90.36
			$\beta_1 = 0.96$	<0.05		
Smooth, 30 mph	$SN_{Av.}$, Run1	$SN_{Av.}$, Run2	$\beta_0 = -0.55$	0.43	0.997	99.42
			$\beta_1 = 1.01$	<0.05		
	$SN_{Av.}$, Run1	$SN_{Av.}$, Run3	$\beta_0 = 0.59$	0.67	0.988	97.53
			$\beta_1 = 0.97$	<0.05		
	$SN_{Peak.}$, Run1	$SN_{Peak.}$, Run2	$\beta_0 = -2.72$	0.31	0.985	96.96
			$\beta_1 = 1.07$	<0.05		
	$SN_{Peak.}$, Run1	$SN_{Peak.}$, Run3	$\beta_0 = 1.97$	0.42	0.984	96.87
			$\beta_1 = 0.96$	<0.05		
Ribbed, 40 mph	$SN_{Av.}$, Run1	$SN_{Av.}$, Run2	$\beta_0 = 2.24$	0.06	0.995	99.01
			$\beta_1 = 0.95$	<0.05		
	$SN_{Av.}$, Run1	$SN_{Av.}$, Run3	$\beta_0 = 1.50$	0.12	0.997	99.29
			$\beta_1 = 0.96$	<0.05		
	$SN_{Peak.}$, Run1	$SN_{Peak.}$, Run2	$\beta_0 = 1.43$	0.80	0.957	91.52
			$\beta_1 = 0.98$	<0.05		
	$SN_{Peak.}$, Run1	$SN_{Peak.}$, Run3	$\beta_0 = 3.69$	0.51	0.955	91.12
			$\beta_1 = 0.95$	<0.05		
Smooth, 40 mph	$SN_{Av.}$, Run1	$SN_{Av.}$, Run2	$\beta_0 = -0.53$	0.78	0.967	93.42
			$\beta_1 = 1.01$	<0.05		
	$SN_{Av.}$, Run1	$SN_{Av.}$, Run3	$\beta_0 = 1.02$	0.60	0.964	92.97
			$\beta_1 = 0.98$	<0.05		
	$SN_{Peak.}$, Run1	$SN_{Peak.}$, Run2	$\beta_0 = 2.77$	0.42	0.952	90.69
			$\beta_1 = 0.91$	<0.05		
	$SN_{Peak.}$, Run1	$SN_{Peak.}$, Run3	$\beta_0 = 1.28$	0.67	0.968	93.64
			$\beta_1 = 0.97$	<0.05		

Figure 31a and Figure 31b show the scatter plot and fitted regression lines of the peak SN and average SN values acquired with the LWST operated at 30 and 40 mph using smooth and ribbed tires versus the MPD acquired using the stationary LTS. Table 13 presents a summary of the regression models fitted to the data shown in Figure 31. The fitted models have the linear form $SN = \beta_0 + \beta_1 MPD$, where SN corresponds the average or peak skid number from tests performed using the ribbed or smooth tire at test speeds of 30 or 40 mph, as indicated in the first column of Table 13. Based on the fact that the significance F values in Table 13 are less than the critical value of 0.05, the regression models including MPD acquired using LTS are statistically

significant at a confidence level of 95%. This means that a model that includes MPD as an explanatory variable is significantly different from a model that uses the mean SN regardless of the different MPD. Moreover, the fact that the p-values are less than 0.05 for the regression coefficient β_1 relating the SNs to MPD in all models indicates that they are significantly different from zero at a 95% confidence level. However, there is insufficient evidence that the intercepts β_0 are different from zero at a 95% confidence level, except for the models describing the peak SN acquired using the ribbed tire. The limited number of observations does not allow for robust conclusions regarding the physical explanation of these models.

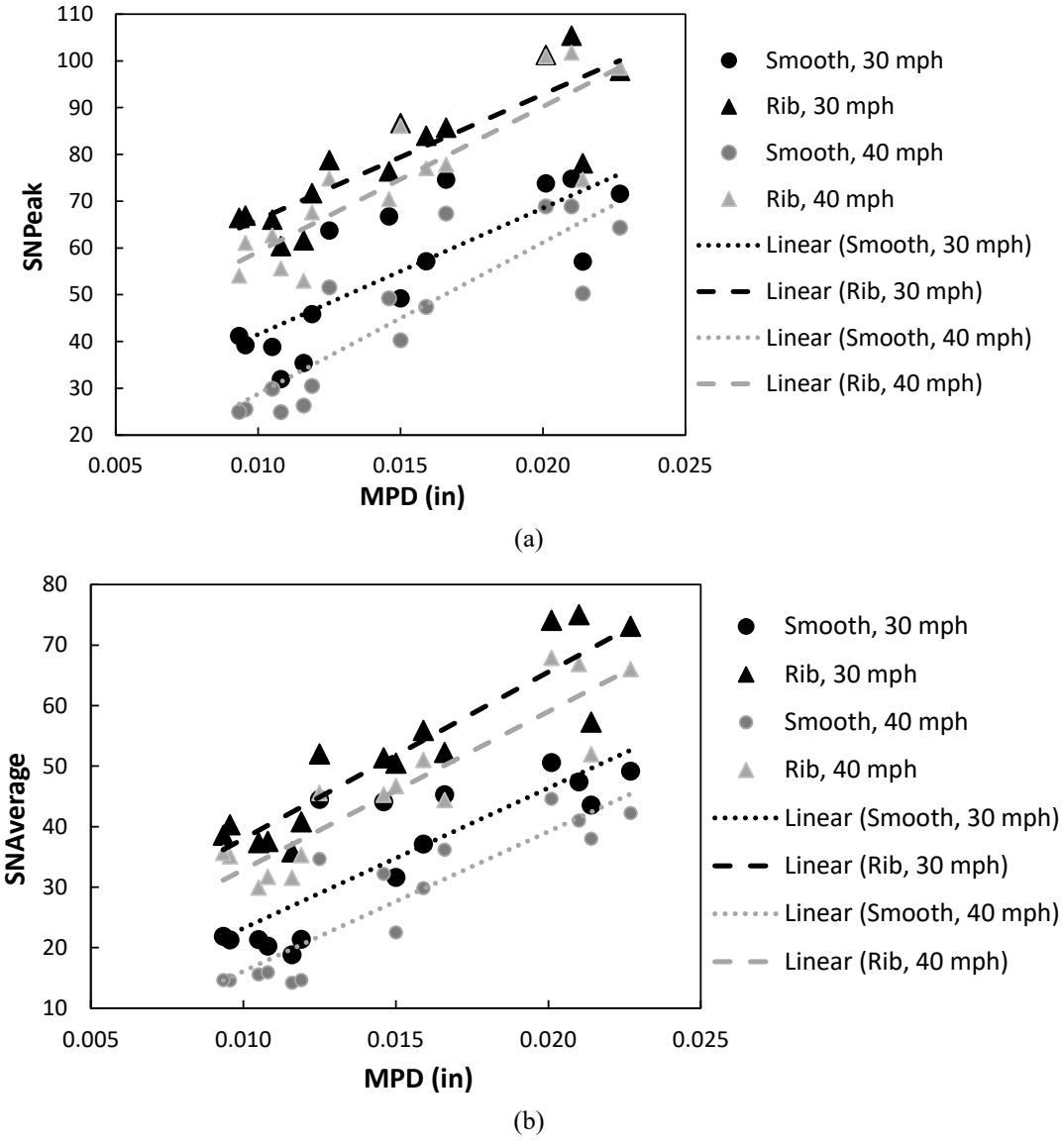

Figure 31. Scatter plots with fitted linear regression models of (a) peak and (b) average SNs versus the MPD values acquired using stationary LTS

Table 13. Summary of regression models between SNs and MPD acquired using the stationary LTS

Model	Parameter	Value	P-value	Correlation Coefficient	R^2 (%)	Sig. F
Peak, Smooth, 30 mph	β_0	14.48	0.12	0.80	63.59	<0.05
	β_1	2702.08	<0.05			
Peak, Ribbed, 30 mph	β_0	39.27	<0.05	0.86	73.43	<0.05
	β_1	2676.89	<0.05			
Peak, Smooth, 40 mph	β_0	-3.58	0.67	0.87	74.78	<0.05
	β_1	3238.17	<0.05			
Peak, Ribbed, 40 mph	β_0	28.16	<0.05	0.86	74.28	<0.05
	β_1	3103.24	<0.05			
Average, Smooth, 30 mph	β_0	0.04	0.99	0.85	72.23	<0.05
	β_1	2317.14	<0.05			
Average, Ribbed, 30 mph	β_0	10.42	0.06	0.92	84.43	<0.05
	β_1	2756.49	<0.05			
Average, Smooth, 40 mph	β_0	-7.01	0.17	0.90	80.69	<0.05
	β_1	2309.20	<0.05			
Average, Ribbed, 40 mph	β_0	6.76	0.20	0.91	83.54	<0.05
	β_1	2612.13	<0.05			

Figure 32a and Figure 32b show the scatter plot and fitted regression lines of the peak SN and average SN values acquired with the LWST operated at 30 and 40 mph using smooth and ribbed tires versus the MPD acquired using the SCRIM operated at 40 mph. Table 14 presents a summary of the regression models fitted to the data shown in Figure 32. Based on the fact that the significance F values in Table 14 are less than the critical value of 0.05, the regression models including MPD acquired using the SCRIM operated at 40 mph are statistically significant at a confidence level of 95%. Moreover, the fact that the p-values are less than 0.05 for the regression coefficient β_1 relating SNs to MPD in all models indicates that they are significantly different from zero at a 95% confidence level. However, there is insufficient evidence that the intercepts β_0 are different from zero at a 95% confidence level. Generally, the correlation coefficients, describing the correlation between the dependent and independent variables, and the coefficients of determination (R^2) are lower when using the MPD acquired using the SCRIM as opposed to the MPD acquired using the stationary LTS. This can be attributed to higher scatter and uncertainty in the SCRIM MPD measurements or the lower number of observations. Models derived using the MPD acquired from the SCRIM operated at 30 and 40 mph resulted in lower correlation coefficients and coefficients of determination.

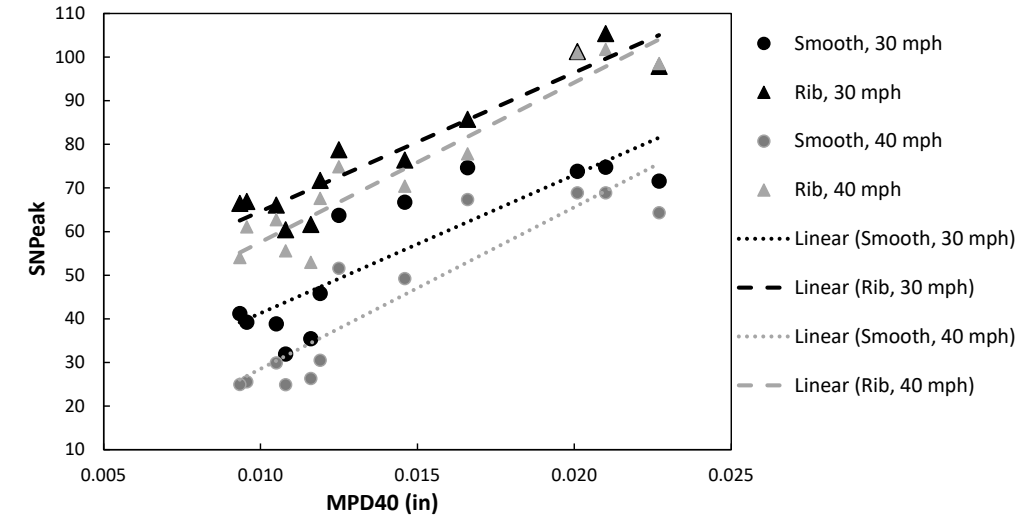

(a)

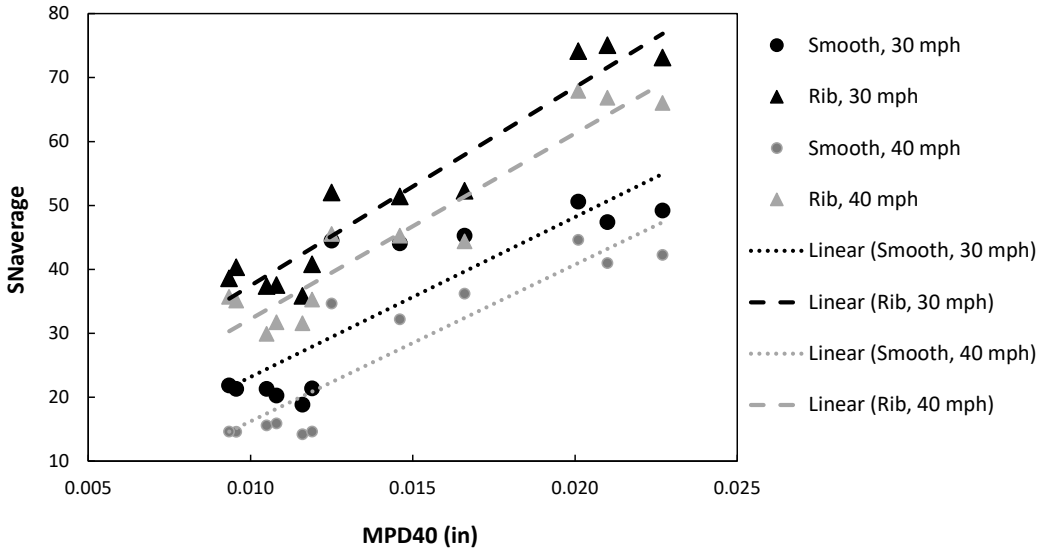

(b)

Figure 32. Scatter plots with fitted linear regression models of (a) peak and (b) average SNs versus the MPD values acquired using the SCRIM at 40 mph

Table 14. Summary of regression models between SNs and MPD acquired using the SCRIM at 40 mph

Model	Parameter	Value	P-value	Correlation Coefficient	R^2 (%)	Sig. F
Peak, Smooth, 30 mph	β_0	-6.54	0.68	0.79	61.81	<0.05
	β_1	3946.99	<0.05			
Peak, Ribbed, 30 mph	β_0	25.93	0.13	0.73	53.92	<0.05
	β_1	3364.01	<0.05			
Peak, Smooth, 40 mph	β_0	-30.49	0.051	0.87	75.50	<0.05
	β_1	4815.32	<0.05			
Peak, Ribbed, 40 mph	β_0	13.41	0.47	0.73	53.63	<0.05
	β_1	3847.02	<0.05			
Average, Smooth, 30 mph	β_0	-17.21	0.16	0.83	68.54	<0.05
	β_1	3284.63	<0.05			
Average, Ribbed, 30 mph	β_0	-0.12	0.99	0.74	54.76	<0.05
	β_1	3270.80	<0.05			
Average, Smooth, 40 mph	β_0	-22.42	0.04	0.86	73.67	<0.05
	β_1	3161.09	<0.05			
Average, Ribbed, 40 mph	β_0	-1.18	0.94	0.70	49.57	<0.05
	β_1	2947.19	<0.05			

Sideway-Force Coefficient Routine Investigation Machine (SCRIM)

Figure 33 presents the acquired SR values and MPD at nominal test speeds of 30, 40, and 50 mph at the control sites. Moreover, the figure shows the uncorrected SR values and the corrected SR values shifted to a test speed 30 mph. The actual speed in the tests operated at a nominal speed of 30 mph was consistently close to 30 mph, which yielded the smallest correction value. Therefore, the corrected SR30 estimated from the SR values acquired at a 30 mph nominal speed was used as the reference measurement in the speed correction evaluation. However, it can be noted that there are considerable differences between the trends in the uncorrected SR values acquired from the same sites at different speeds. Negative SR values were considered as errors in the measurement and removed from the readings acquired at 40 mph from site 4, as shown in Figure 33h. Except for the negative values at site 4, sites 4 and 6 show the lowest fluctuation in the SR measurements along the test segments and at different speeds. Figure 33 shows some peaks and valleys in the SR readings that amplify or attenuate at different test speeds at the same site. However, there are some abrupt changes in the SR measurements. For example, at site 2 at a distance of 2,700 ft, the SR measurements acquired at 30 mph changed from 51 to 25 around 2,700 ft, while in the same location, the SR measurements acquired at 40 mph changed from 66 (highest value) to 37, as shown in Figure 33e.

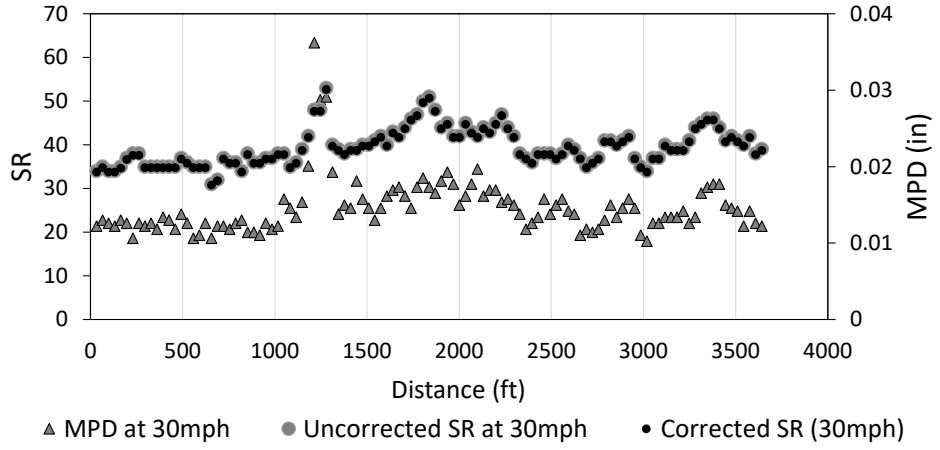

(a) SCRIM reading and MPD at a nominal speed of 30 mph at site 1

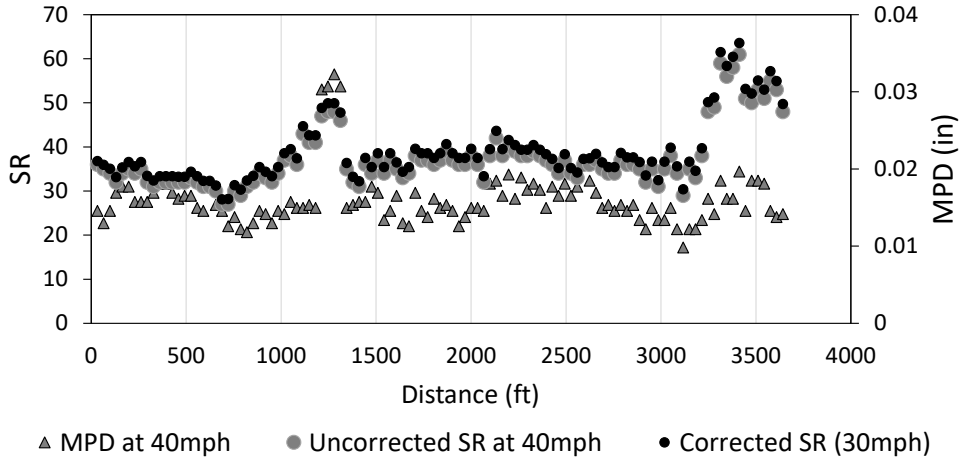

(b) SCRIM reading and MPD at a nominal speed of 40 mph at site 1

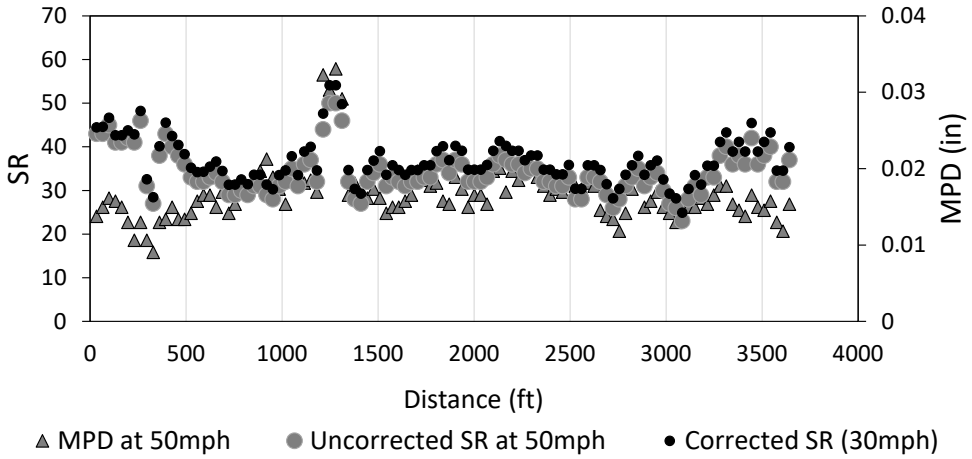

(c) SCRIM reading and MPD at a nominal speed of 50 mph at site 1

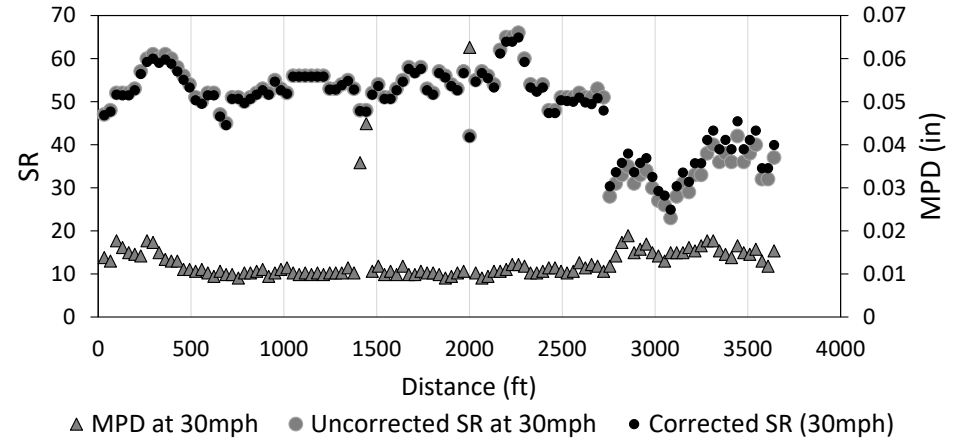

(d) SCRIM reading and MPD at a nominal speed of 30 mph at site 2

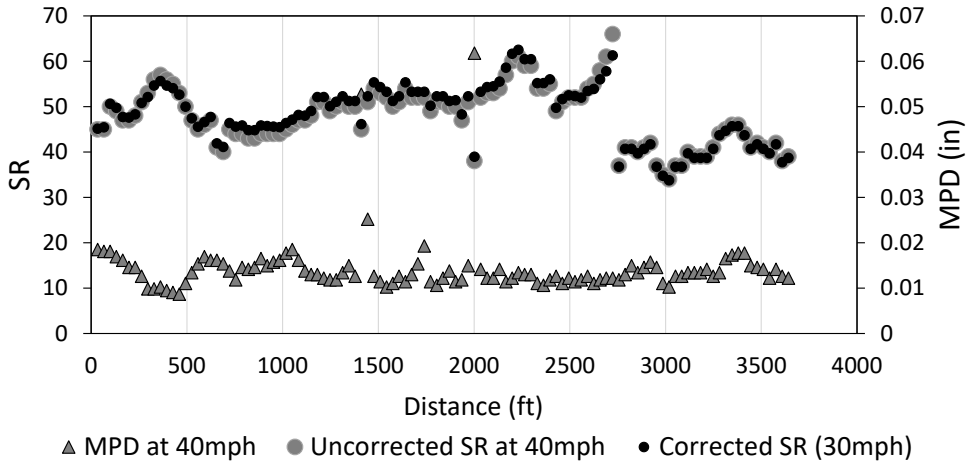

(e) SCRIM reading and MPD at a nominal speed of 40 mph at site 2

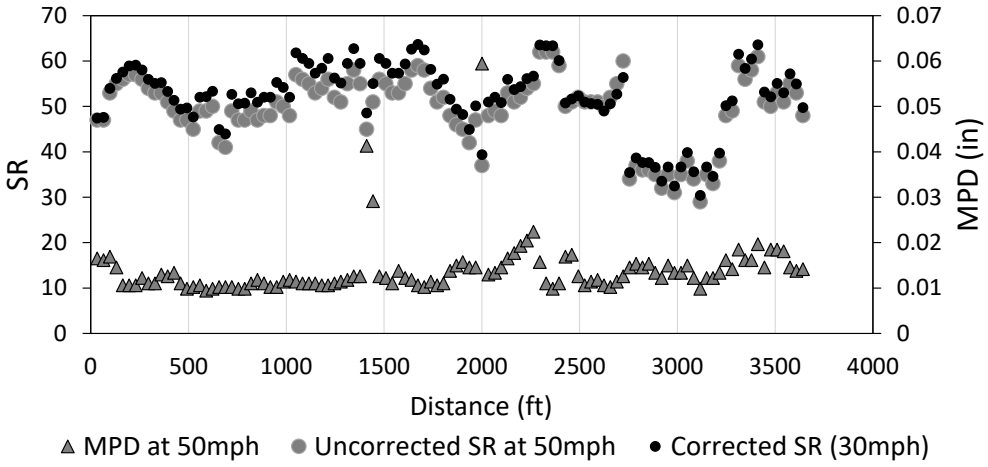

(f) SCRIM reading and MPD at a nominal speed of 50 mph at site 2

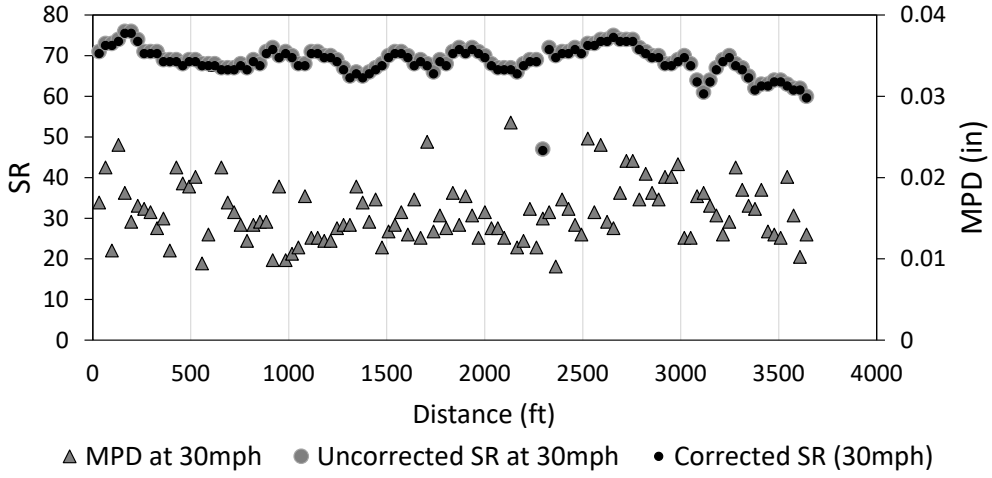

(g) SCRIM reading and MPD at a nominal speed of 30 mph at site 4

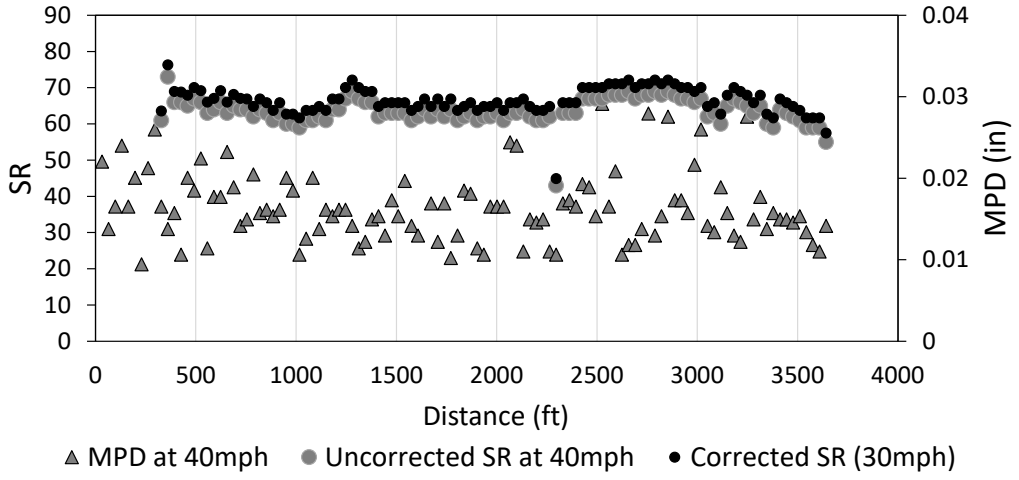

(h) SCRIM reading and MPD at a nominal speed of 40 mph at site 4

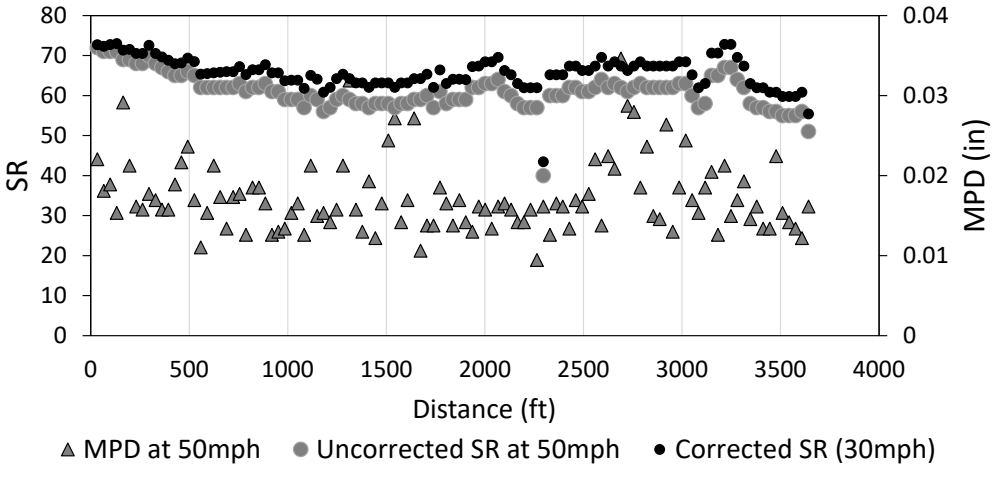

(i) SCRIM reading and MPD at a nominal speed of 50 mph at site 4

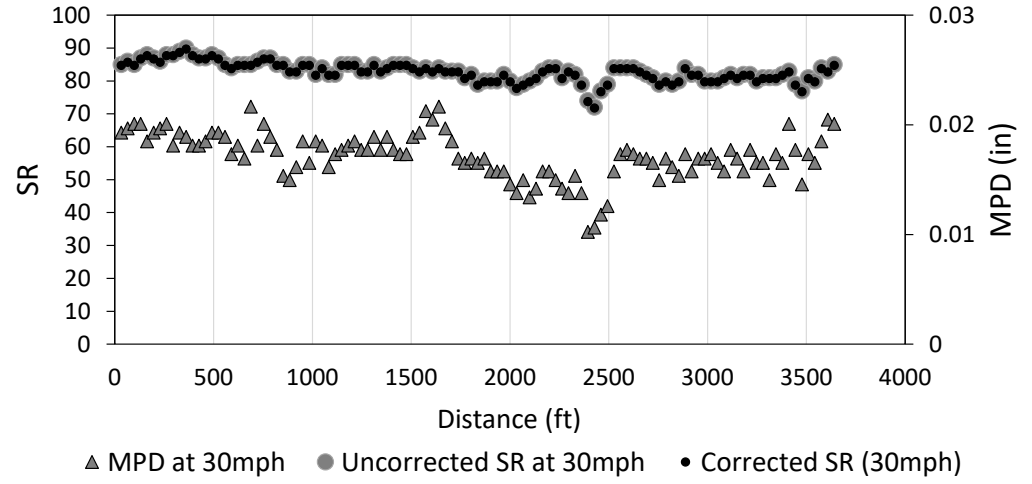

(j) SCRIM reading and MPD at a nominal speed of 30 mph at site 6

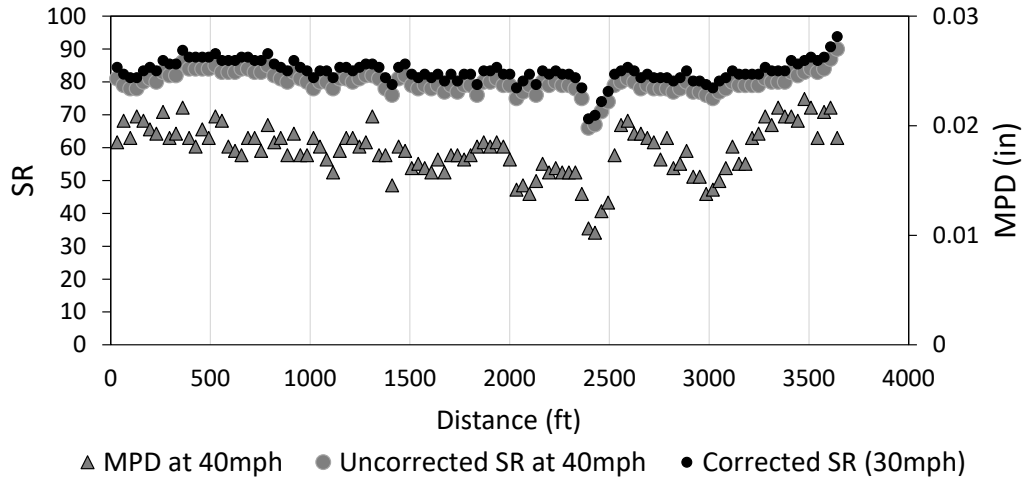

(k) SCRIM reading and MPD at a nominal speed of 40 mph at site 6

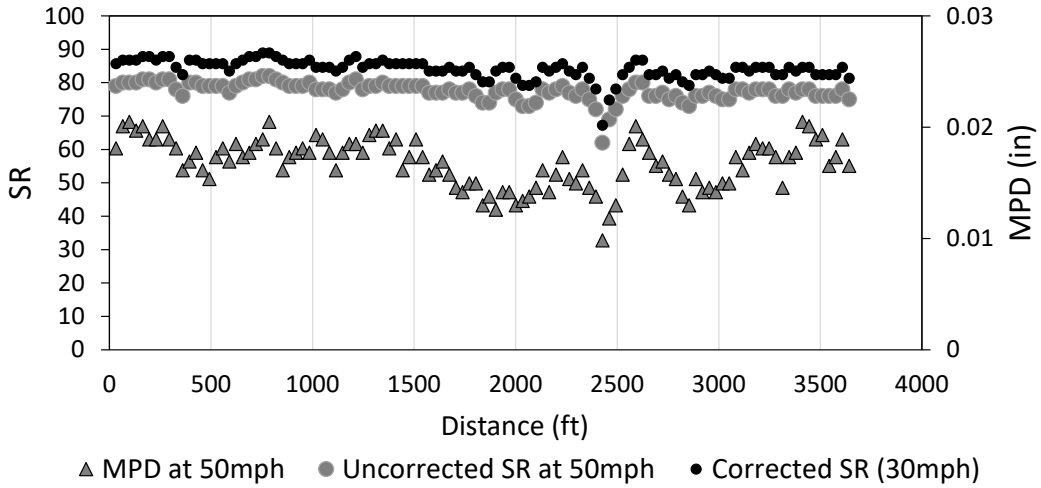

(l) SCRIM reading and MPD at a nominal speed of 50 mph at site 6

Figure 33. SCRIM readings at 30, 40, and 40 mph and MPD (in) measurements acquired at the corresponding speeds from sites 1, 2, 4, and 6

To test the quality of the speed correction formula presented above, the corrected measurements of SR30 estimated from the measurements of SR(v) acquired at nominal speeds (v) of 40 and 50 mph were plotted against the SR30 measurements acquired at a nominal test speed of 30 mph from the four control sites, as shown in Figure 34. It should be emphasized that the speed used in the correction equation was the actual recorded speed in km/h and not the nominal test speed. Moreover, the regression equations presented in Table 15 show the linear regression models that correlate the corrected measurements to the measurements acquired at 30 mph. The correlations between the SR30 measurements acquired at a nominal test speed of 30 mph and the SR30 measurement acquired at other nominal test speeds are statistically significant at a 95% confidence level, as indicated by the significance F values less than 0.05. The significance F is the p-value corresponding to the ANOVA test for regression model significance. Although the models are statistically significant, they have high scatter (i.e., uncertainty) around their regression line, bias from the line of equality, and different regression models across different sites. This limits the ability to correct/transfer the measurements acquired at different speeds to a common reference scale.

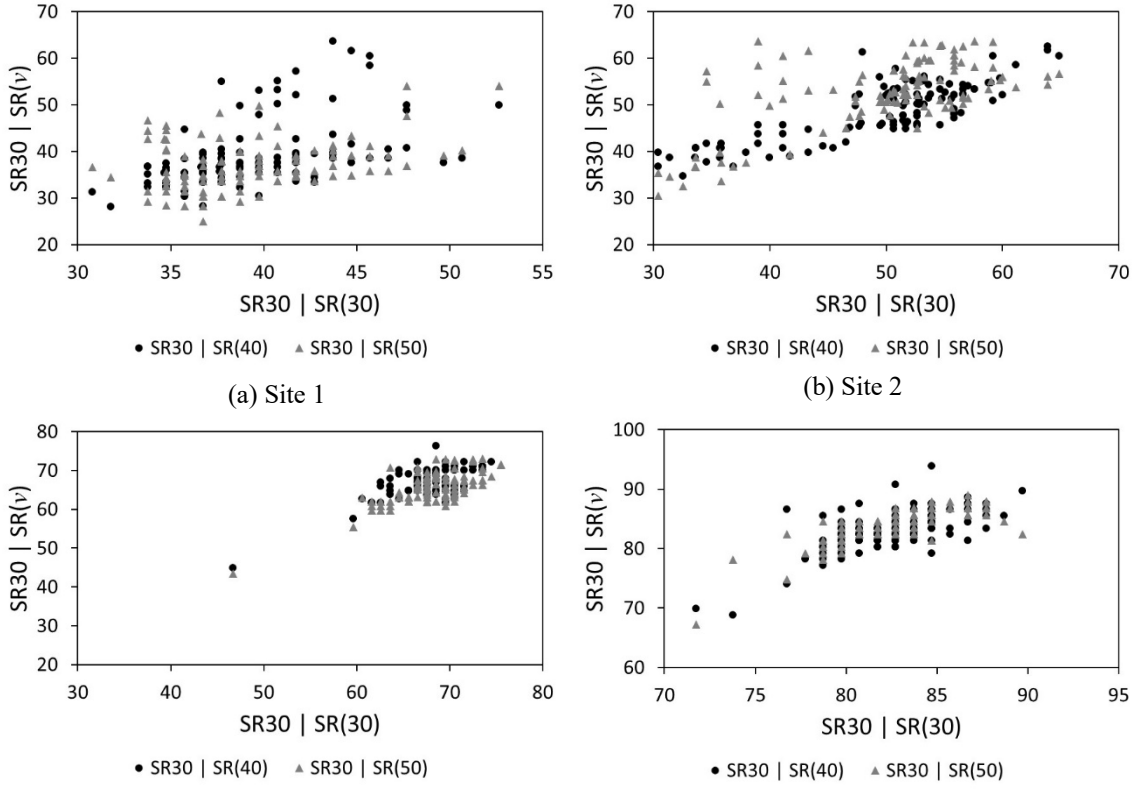

(a) Site 1 (b) Site 2

(c) Site 4 (d) Site 6

Figure 34. Speed-corrected measurements of SR30 based on measurements acquired at 40 and 50 mph versus SR30 based on measurements acquired at 30 mph for different sites

Theoretically, the corrected measurements and measurements acquired at 30 mph should match. However, the variability in the spatial location of the measurements from the different tests, the variability and uncertainty in the measured values, and the uncertainty in the speed correction

equation all attribute to the variability observed in the regression models for SR30 from different tests.

Table 15. Linear regression models relating SR30 estimated from measurements acquired at nominal test speeds of 40 and 50 mph to SR30 estimated from measurements acquired at a nominal test speed of 30 mph

Site	Nominal Speed (mph)	Parameter	Value	P-Value	Correlation Coefficient	R^2 (%)	Sig. F
1	40	β_0	20.11	<0.05	0.34	11.82	<0.05
		β_1	0.43	<0.05			
	50	β_0	3.91	0.48	0.52	27.16	<0.05
		β_1	0.89	<0.05			
2	40	β_0	17.71	<0.05	0.85	71.5	<0.05
		β_1	0.63	<0.05			
	50	β_0	21.90	<0.05	0.69	47.03	<0.05
		β_1	0.62	<0.05			
4	40	β_0	23.00	<0.05	0.63	39.59	<0.05
		β_1	0.64	<0.05			
	50	β_0	14.87	<0.05	0.71	50.00	<0.05
		β_1	0.75	<0.05			
6	40	β_0	18.58	<0.05	0.67	45.06	<0.05
		β_1	0.78	<0.05			
	50	β_0	20.46	<0.05	0.78	60.92	<0.05
		β_1	0.77	<0.05			

Table 16 presents the average ($\overline{SR}$) and standard deviation ($\hat{\sigma}_{SR}$) of the uncorrected SR values acquired at nominal test speeds of 30, 40, and 50 mph. The SR measurements were acquired at different spatial locations along the test sites and at fluctuating actual speeds deviating from the nominal test speed. Therefore, the variability in the measurements, represented by the standard deviation, is composed of the spatial variability component and the measurement variability and uncertainty. Due to the lack of a standard model to quantify the ground truth measurement of friction, it is not possible with the limited data available to quantify the magnitude of each component of these variabilities.

Table 16. Summary statistics of uncorrected SR values acquired at nominal test speeds of 30, 40, and 50 mph across the control sites

Site	Nominal Speed	$\overline{SR}$	$\hat{\sigma}_{SR}$
1	30	39.57	4.27
	40	37.43	7.00
	50	34.15	5.06
2	30	48.91	8.74
	40	47.84	6.41
	50	49.52	7.48
4	30	68.76	3.85
	40	63.64	3.61
	50	61.05	4.44
6	30	82.92	3.02
	40	79.82	3.37
	50	77.50	2.74

To evaluate the correlation between SR30 and MPD acquired from the SCRIM, regression models were derived for the data acquired from the four sites and at three nominal test speeds separately. SR30 was used since it was proposed as a reference value by the manufacturer. Figure 35 shows that there is great scatter in the SR30 values relative to the spread of the MPD values at sites 1 and 2, while the SR30 values had a lower spread at sites 4 and 6. Table 17 shows that the regression models had varying ranges of model parameters and summary statistics. More specifically, the models derived for site 2 had a negative slope parameter, indicating that the higher the MPD value, the lower friction. This can be a product of the influential points appearing in Figure 35 with MPD values greater than 0.02, which appear in Figure 33c near 1,500 and 2,000 ft. These extreme values can be due to measurement error or an isolated feature on the road surface skewing the MPD measurements. It should be emphasized that MPD is not the only friction characterization parameter. In fact, MPD is a sensitive parameter that can be affected by anomalies and isolated surface features that do not necessarily relate to friction. Therefore, the correlation models reported in Table 17 can be influenced by many variables driving both measurements, including systematic measurement errors. The reported correlations should not be treated as engineering models describing the physical mechanism unless there is another scientific reason for that assumption.

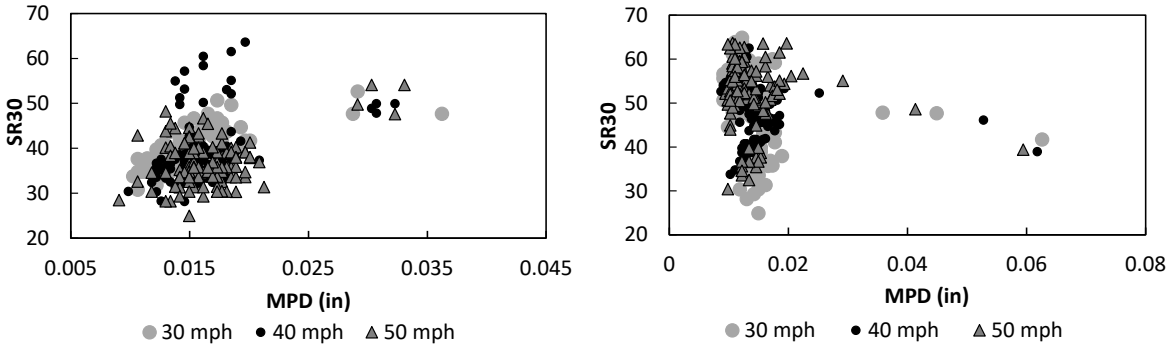

(a) Site 1

(b) Site 2

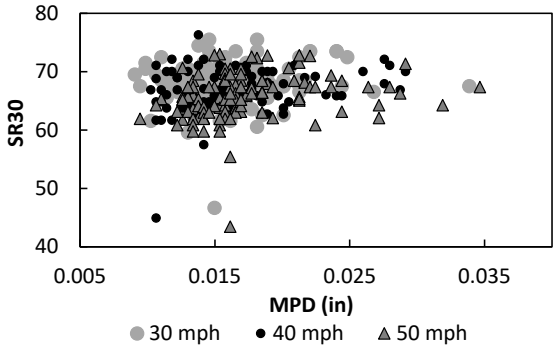

(c) Site 4

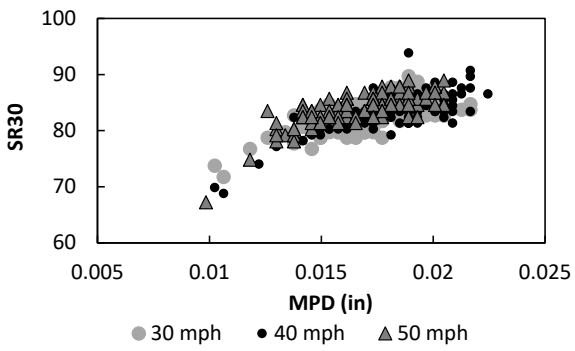

(d) Site 6

Figure 35. SR30 versus MPD from measurements acquired at nominal test speeds of 30, 40, and 50 mph at different sites

Table 17. Linear regression models relating SR30 to MPD estimated from measurements acquired at nominal test speeds of 30, 40, and 50 mph

Site	Nominal Speed (mph)	Parameter	Value	P-Value	Correlation Coefficient	R^2 (%)	Sig. F
1	30	β_0	27.05	<0.05	0.72	51.81	<0.05
		β_1	838.07	<0.05			
	40	β_0	26.05	<0.05	0.39	15.22	<0.05
		β_1	807.85	<0.05			
	50	β_0	26.38	<0.05	0.43	18.67	<0.05
		β_1	626.15	<0.05			
2	30	β_0	53.58	<0.05	0.27	7.00	<0.05
		β_1	-353.19	<0.05			
	40	β_0	51.40	<0.05	0.21	4.41	<0.05
		β_1	-213.04	<0.05			
	50	β_0	54.61	<0.05	0.14	2.00	0.14
		β_1	-183.56	0.14			
4	30	β_0	66.93	<0.05	0.09	0.81	0.35
		β_1	86.09	0.35			
	40	β_0	63.27	<0.05	0.23	5.14	<0.05
		β_1	201.66	<0.05			
	50	β_0	62.30	<0.05	0.22	5.00	<0.05
		β_1	197.22	<0.05			
6	30	β_0	64.94	<0.05	0.73	52.64	<0.05
		β_1	1030.17	<0.05			
	40	β_0	62.80	<0.05	0.76	58.08	<0.05
		β_1	1147.22	<0.05			
	50	β_0	66.56	<0.05	0.76	58.29	<0.05
		β_1	1040.87	<0.05			

Correlation between SCRIM and BPT measurements

This section presents the result of an analysis contrasting the SCRIM measurements with the BPT measurements. To match the dense SCRIM profile to the point BPT readings, the SR values acquired using the SCRIM at the closest point to the stationary BPT, the point before it, and the point after it were averaged and compared to the average BPN acquired using repeated measurements at the same location. Each control site included three stationary locations for the BPT. Figure 36a presents the scatter plot of the average uncorrected SCRIM readings acquired at the three nominal speeds of 30, 40, and 50 mph at the three points for all control sites. Additionally, Figure 36b presents the scatter plot of the average corrected SR30 for the readings acquired at all control sites at the three nominal tests speeds. It is clear from both plots that there is a positive trend around the line of equality between the BPN and the corrected and uncorrected SCRIM readings acquired at all speeds.

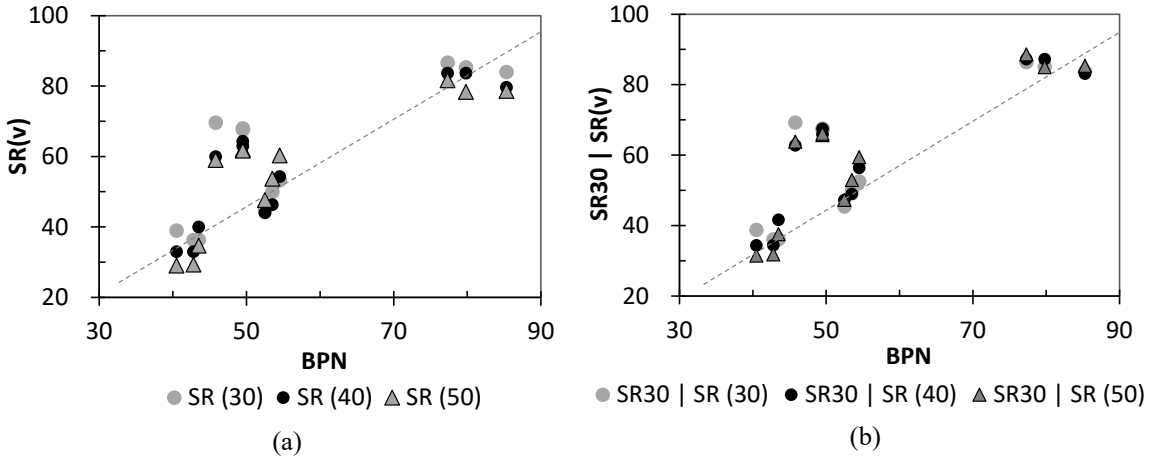

Figure 36. SCRIM measurements acquired at the three nominal speeds plotted against the BPN: (a) uncorrected SCRIM readings and (b) SCRIM readings corrected to 30 mph

Table 18 presents linear regression models correlating corrected and uncorrected SR measurements (the dependent variable) to BPN (the independent variable). It can be noticed that all models are statistically significant with a relatively high coefficient of determination. Moreover, Table 18 shows that all of the intercepts in the linear models are statistically insignificant and that the slopes are statistically significant with a value close to one at a 95% confidence level. This indicates that correlations between the BPN and SCRIM measurements are close to one-to-one correspondences. Moreover, this indicates that the SCRIM measurements are related to low-speed friction, which does not necessarily imply that it does not capture the high-speed friction values.

Table 18. Linear regression models correlating corrected and uncorrected SCRIM measurements to BPN

SR	Nominal Speed (mph)	Parameter	Value	P-Value	Correlation Coefficient	R^2 (%)	Sig. F
Corrected (SR30)	30	β_0	2.85	0.83	0.82	67.58	<0.05
		β_1	1.01	<0.05			
	40	β_0	-0.23	0.98	0.86	74.35	<0.05
		β_1	1.07	<0.05			
	50	β_0	-3.66	0.77	0.87	74.86	<0.05
		β_1	1.13	<0.05			
Uncorrected SR (*v*)	30	β_0	3.08	0.82	0.82	66.92	<0.05
		β_1	1.01	<0.05			
	40	β_0	-0.58	0.96	0.86	74.28	<0.05
		β_1	1.03	<0.05			
	50	β_0	-0.78	0.95	0.86	73.45	<0.05
		β_1	1.02	<0.05			

Correlation between SCRIM and LWST measurements

This section presents the results of an analysis contrasting the SCRIM measurements with the LWST measurements. To spatially match the LWST with the SCRIM measurements, the SCRIM readings falling within the LWST skid were averaged and compared to the SN acquired from the same LWST skid. Figure 37a presents a scatter plot of the corrected SCRIM values versus the average SN values acquired at 30 mph using a smooth tire. Figure 37b presents a scatter plot of the corrected SCRIM values versus the peak SN values acquired at 30 mph using a smooth tire. It can be noticed that the peak SN values are more spread out, forming a clearer trend line. Additionally, Figure 37c and Figure 37d present scatter plots of the corrected SCRIM measurements versus the average and peak SN, respectively, acquired using a ribbed tire at 30 mph. Similar to the data acquired using a smooth tire, the peak SN values acquired using a ribbed tire are more spread out compared to the average SN, forming a clearer positive trend line.

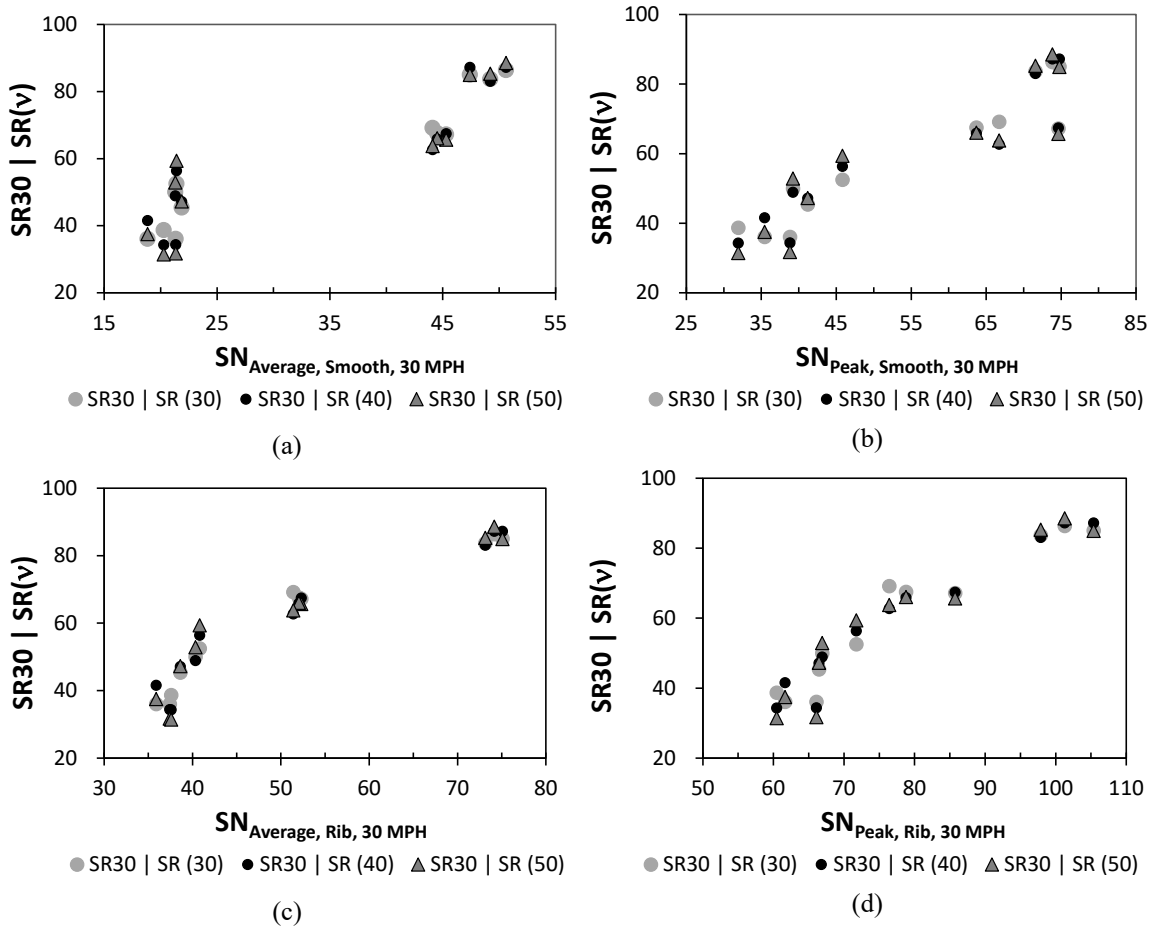

Figure 37. Corrected SCRIM measurements acquired at the three nominal speeds plotted against (a) average SN and (b) peak SN acquired using a smooth tire at 30 mph and (c) average SN and (d) peak SN acquired using a ribbed tire at 30 mph

Table 19 presents linear regression models correlating the corrected SR measurements (the dependent variable) to the average and peak SN values acquired using smooth and ribbed tires at

30 mph. It can be noticed that all models are statistically significant at a 95% confidence level with a relatively high coefficient of determination. The coefficient of determination and correlation coefficient are higher for models derived using the peak SN values. This can be attributed to the fact that the SCRIM readings represent friction at lower speeds. Moreover, the LWST measurements acquired using the ribbed tire are better correlated to the SCRIM measurements. It should be mentioned that the scatter plots for the ribbed tire measurements may represent a nonlinear trend. However, there is insufficient data to derive higher-order correlations.

Table 19. Linear regression models correlating corrected SCRIM measurements to LWST measurements acquired at 30 mph

Tire	Nominal Speed (mph)	Parameter	Value	P-Value	Correlation Coefficient	R^2 (%)	Sig. F
Smooth Average	30	β_0	15.05	<0.05	0.95	89.80	<0.05
		β_1	1.32	<0.05			
	40	β_0	16.62	<0.05	0.91	82.63	<0.05
		β_1	1.27	<0.05			
	50	β_0	15.42	0.08	0.89	78.44	<0.05
		β_1	1.30	<0.05			
Smooth Peak	30	β_0	2.49	0.70	0.95	89.86	<0.05
		β_1	1.05	<0.05			
	40	β_0	3.33	0.66	0.93	86.37	<0.05
		β_1	1.03	<0.05			
	50	β_0	1.62	0.86	0.91	82.53	<0.05
		β_1	1.06	<0.05			
Ribbed Average	30	β_0	-1.17	0.85	0.96	92.01	<0.05
		β_1	1.20	<0.05			
	40	β_0	-1.37	0.82	0.96	91.77	<0.05
		β_1	1.20	<0.05			
	50	β_0	-3.21	0.69	0.94	87.70	<0.05
		β_1	1.24	<0.05			
Ribbed Peak	30	β_0	-30.60	<0.05	0.96	91.35	<0.05
		β_1	1.16	<0.05			
	40	β_0	-32.24	<0.05	0.97	93.91	<0.05
		β_1	1.18	<0.05			
	50	β_0	-34.75	<0.05	0.95	89.40	<0.05
		β_1	1.21	<0.05			

In addition to the correlation between the corrected SCRIM measurements and LWST measurements acquired at 30 mph, Figure 38 presents scatter plots of the uncorrected SCRIM measurements acquired at 40 mph versus the average and peak SN acquired at 40 mph using smooth and ribbed tires. From Figure 38, it is clear that there is a nonlinear positive trend. However, due to the limited number and range of observations, it is difficult to derive nonlinear correlations between the measurements. Table 20 presents linear regression models correlating

the uncorrected SCRIM measurements to the LWST measurements acquired at 40 mph. All of the linear regression models are statistically significant at a 95% confidence level with a relatively high coefficient of determination.

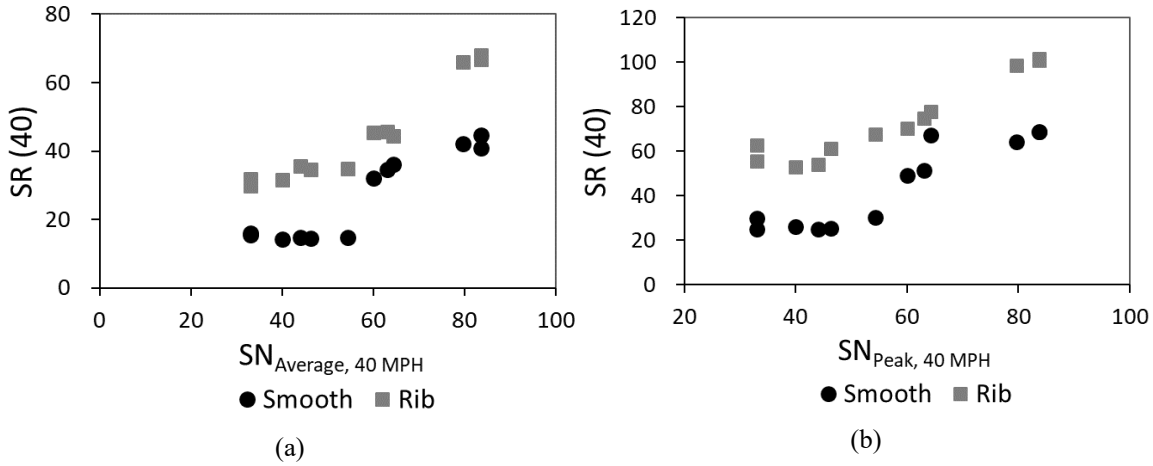

Figure 38. Uncorrected SCRIM measurements acquired at 40 mph versus (a) average SN acquired at 40 mph using smooth and ribbed tires and (b) peak SN acquired at 40 mph using smooth and ribbed tires

Table 20. Linear regression models correlating uncorrected SCRIM measurements to LWST measurements acquired at 40 mph

SN	tire	Parameter	Value	P-Value	Correlation Coefficient	R^2 (%)	Sig. F
Average	Smooth	β_0	-9.70	0.08	0.93	85.80	<0.05
		β_1	0.64	<0.05			
	Rib	β_0	1.53	0.72	0.96	92.10	<0.05
		β_1	0.75	<0.05			
Peak	Smooth	β_0	-10.20	0.21	0.92	85.04	<0.05
		β_1	0.96	<0.05			
	Rib	β_0	19.87	<0.05	0.95	90.72	<0.05
		β_1	0.94	<0.05			

Curves and Miscellaneous Network Segments

Figure 39 shows the acquired SR values for the four HFST curves included in the study. The data recording began ahead of the actual curve and continued after the curve to capture and contrast the difference in the SR values between the typical pavement surfaces tangent to the curves and the HFST. The test speed fluctuated between 23.5 and 26 mph at all test sites. The intent was to obtain comparable friction measurements across the curves. It can be noted in Figure 39a, b, and d that curves HFST1, HFST2, and HFST3 had somewhat similar trends, with a relatively smooth record featuring long wave fluctuations and an isolated significantly high-friction measurement segment between 4,000 and 6,000 ft corresponding to the HFST surface. Relatively low

fluctuations are expected in friction measurements at short distances. Curve HFST3, shown in Figure 39c, had a lower average SR value and slightly higher level of variability at a short distance compared to the other curves.

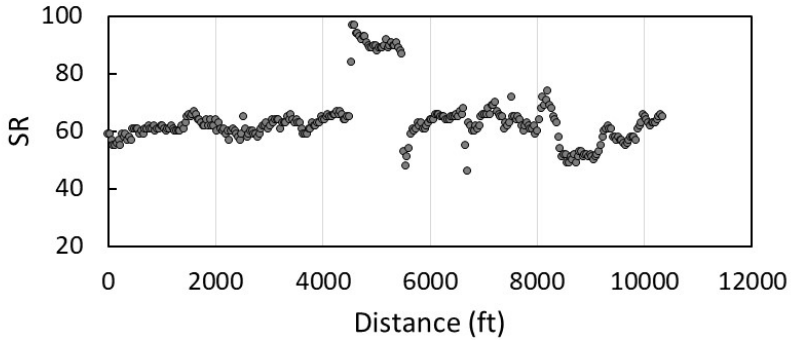

(a) HFST1

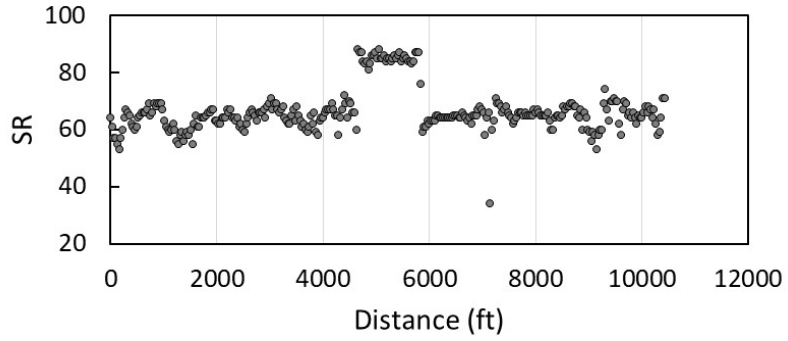

(b) HFST2

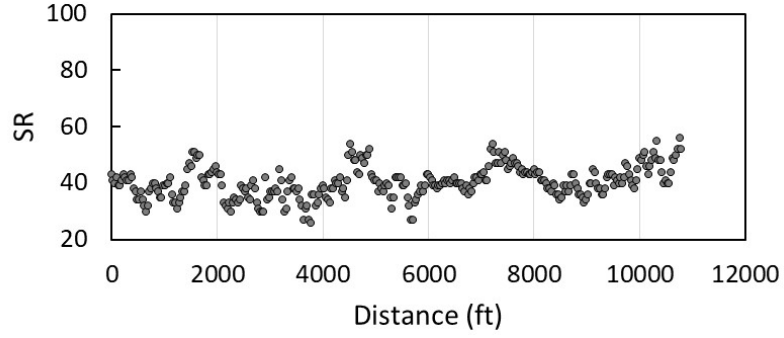

(c) HFST3

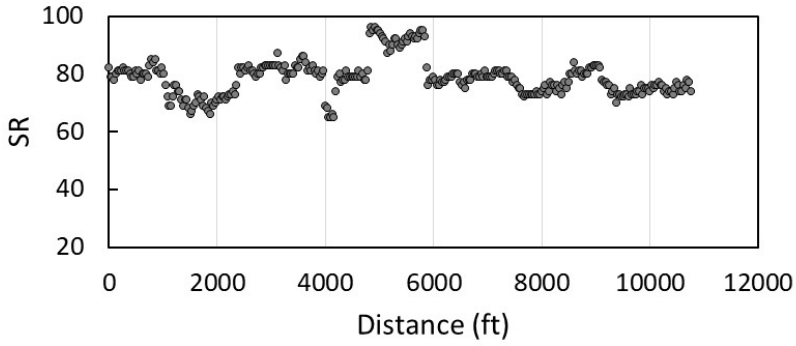

(d) HFST4

Figure 39. SCRIM readings acquired at prevailing traffic speed from curves HFST1 through HFST4

Figure 40 presents the SR readings acquired from 4 of the other 11 curves included in the study with four distinct surface types. From Figure 40 a, b, and d, it can be noted that there are some significant fluctuations in the measurements, which can be due to actual variations in the surface characteristics or fluctuations in the measuring system. As mentioned earlier, it is not possible to identify the source of variability due to the lack of independent ground truth measurements. It should be emphasized again that the measurements have a spatial nature, and therefore the standard deviation and average values should not be interpreted with the typical statistical understanding of repeated and independent observations of the same process.

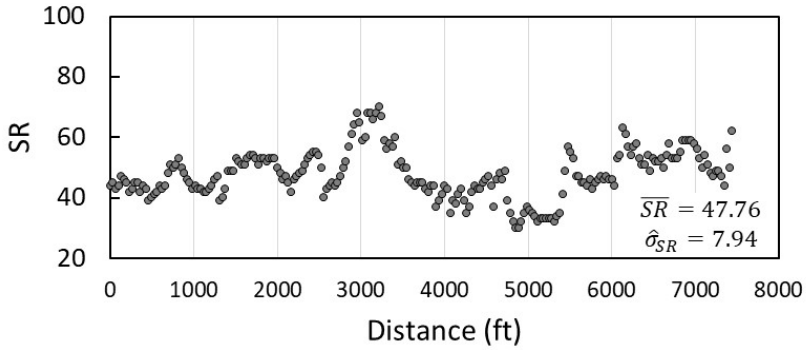

(a) C1

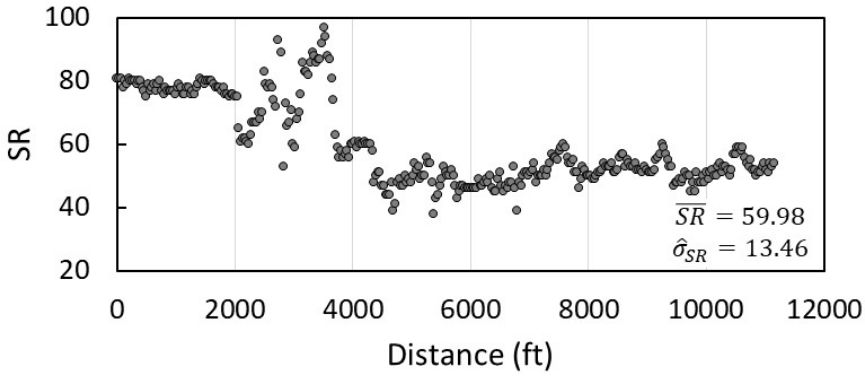

(b) C2

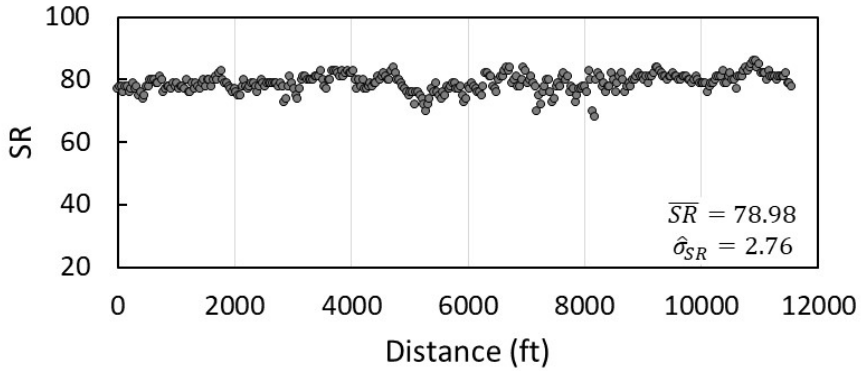

(c) C3

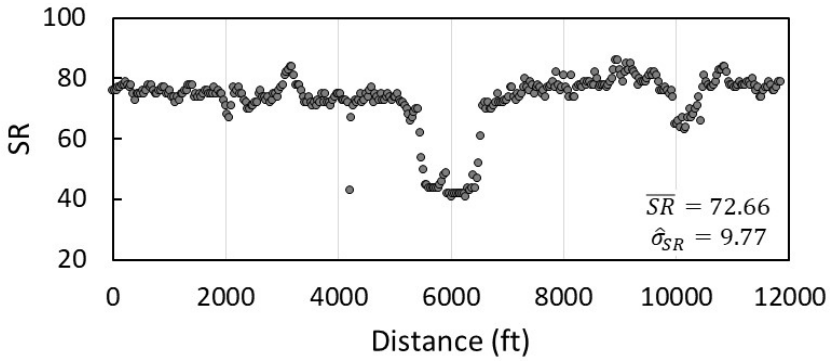

(d) C4

Figure 40. SCRIM readings acquired at prevailing traffic speed from curves C1 through C4

Figure 41 presents the SCRIM readings along the four miscellaneous sites. From the figure, it can be noticed that there are two levels of spatial variability: variability at a short distance and global variability at a long range. Therefore, the variability in the measurements can be divided into three major sources: local fluctuations, short-range spatial variability, and long-range spatial variability (trend). The measurement fluctuations can be attributed to variability in speed, variability in tire condition such as temperature, and errors in the data acquisition. The short-range spatial variability can be attributed to variations in the surface properties within the same segment. Finally, the long-range spatial variability can be attributed to changes in the surface type or traffic condition that affect the polishing of the surface at different locations.

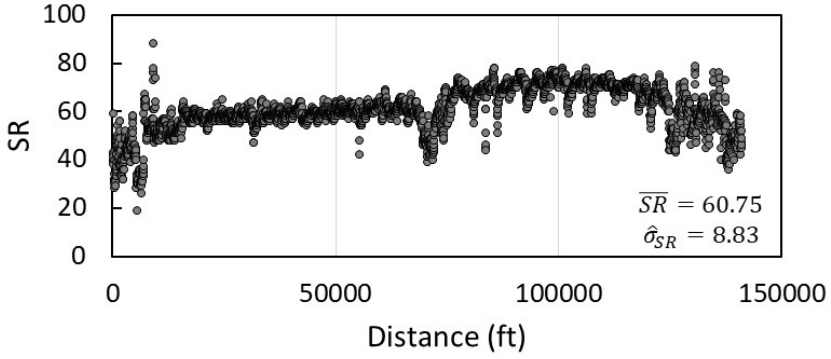

(a) Mis1

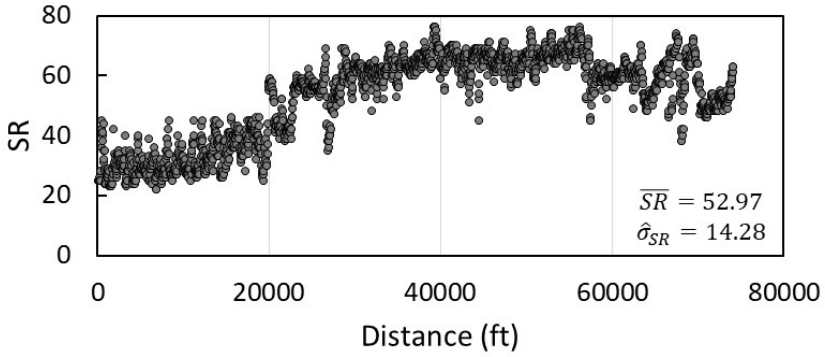

(b) Mis2

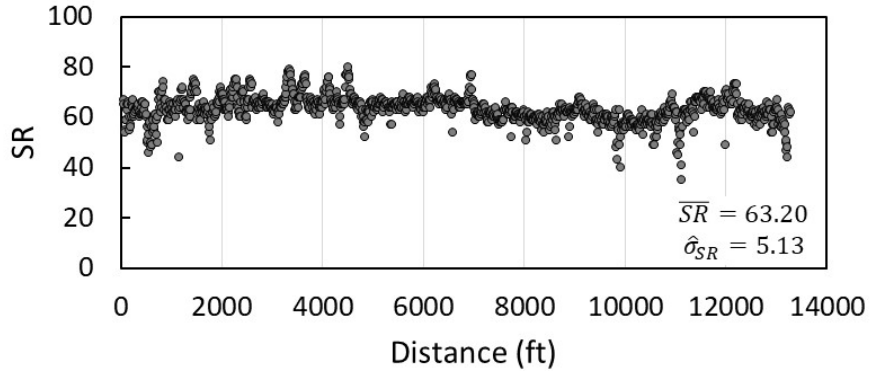

(c) Mis3

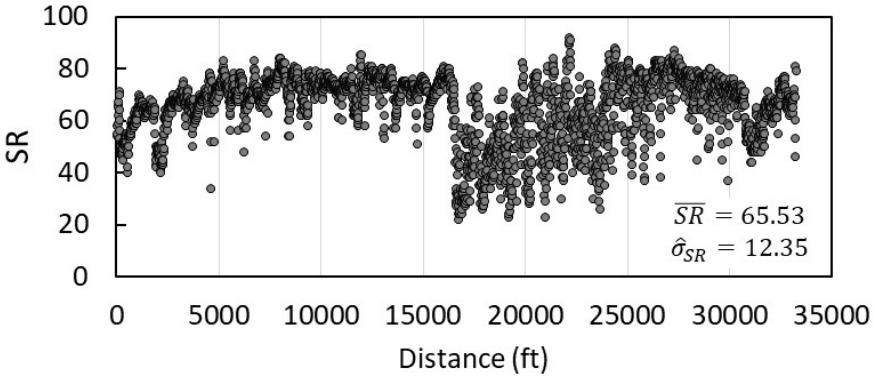

(d) Mis4

Figure 41. SCRIM readings acquired at prevailing traffic speed from curves Mis1 through Mis4

CONCLUSIONS

This report presented the findings from a field testing program designed to initially evaluate selected CFME technologies in concert with the LWST currently available at the Iowa DOT. A wide range of devices were used to acquire friction and texture measurements, including stationary LTS, DFT, BPT, LWST, and SCRIM.

The conclusions of this study are presented below. It should be noted that these conclusions are based on the limited number of test surfaces included in this study and should not be extrapolated to describe other surfaces and testing conditions. More specifically, the developed correlations are empirical in nature and do not capture a fundamental model describing the behavior of the various devices on the pavement surfaces.

The conclusions of this study are as follows:

- The texture measurements acquired using the SCRIM and reported as MPD values varied with varying speeds when acquired on the same surface.
- There was a statistically significant correlation between the BPN and MPD values acquired using the stationary LTS and a significant but sparser correlation (lower R^2) with the MPD values acquired using the SCRIM at a nominal speed of 40 mph.
- There was a statistically significant correlation between the COF values acquired at 30 and 40 mph using the DFT and the MPD values acquired using the stationary LTS and a significant but sparser correlation (lower R^2) with the MPD values acquired using the SCRIM at a nominal speed of 40 mph.
- The LWST measurements were highly repeatable across the control tangent segments.
- The peak SN values acquired using the LWST were more spread out compared to the average SN values when correlated to the MPD values acquired using the stationary LTS and the SCRIM at a nominal speed of 40 mph. This may indicate that the peak SN can be more sensitive to the MPD values acquired in this study.
- The SCRIM acquired friction measurements at a high rate and under varying conditions and road geometries, which can be advantageous for network-level data collection.
- The speed correction equation available to shift the measurements acquired at different speeds to a standard reference value had uncertainty and bias, which should be improved in future studies to ensure consistent reference readings that can be uniformly used in safety analysis.
- There is a significant and strong correlation between the SCRIM measurements and BPN, indicating that the SCRIM can capture low-speed friction.
- There is a significant and strong correlation between the corrected SCRIM measurements (SR30) and the LWST measurements acquired at 30 mph using the smooth and ribbed tires. This indicates that the SCRIM measurements could capture the fully locked friction values.
- There is a significant correlation between the uncorrected SCRIM measurements acquired at a nominal speed of 40 mph and the LWST measurements acquired at 40 mph using smooth and ribbed tires. It should be noted that the scatter plots showed a nonlinear trend between the measurements. However, due to the limited number and range of measurements, it is not feasible to derive nonlinear correlations.

- The SCRIM friction measurements had three sources of variability: measurement uncertainty, short-range spatial variability, and long-range spatial variability (trend), which should be investigated further to quantify the magnitude of these different sources of variability.
- Understanding the sources of variability will be critical for using the SCRIM data in safety evaluations because the current safety analysis method assumes deterministic and consistent explanatory variables across the analysis segment. This variability can be understood with more detailed and robust statistical modeling.
- Overall, the SCRIM presents a promising tool to acquire friction measurements at the network level. However, there is a need for further investigation to better understand the measuring mechanism and develop a robust procedure to handle the data in safety analyses, especially given the spatial nature of the data.

REFERENCES

Anfosso-Ledee, F., P. Nitsche, G. Schwalbe, R. Spielhofer, P. Saleh and B. Wasser. 2009. *Deliverable D06. Report on Policies and Standards Concerning Skid Resistance, Rolling Resistance and Noise Emissions*. Coordination Action FP7-217920. Seventh Framework Programme Theme 7: Transport. Tyre and Road Surface Optimisation for Skid Resistance and Further Effects (TYROSAFE).

de León Izeppi, E., S. W. Katicha, G. W. Flintsch, R. McCarthy, and K. K. McGhee. 2016a. *Continuous Friction Measurement Equipment As a Tool for Improving Crash Rate Prediction: A Pilot Study*. Final Report VTRC 16-R8. Virginia Center for Transportation Innovation and Research, Charlottesville, VA.

de León Izeppi, E., S. W. Katicha, G. W. Flintsch, and K. K. McGhee. 2016b. Pioneering Use of Continuous Pavement Friction Measurements to Develop Safety Performance Functions, Improve Crash Count Prediction, and Evaluate Treatments for Virginia Roads. *Transportation Research Record: Journal of the Transportation Research Board*, Vol. 2583, pp. 81–90.

FHWA. 2010. *Pavement Friction Management*. Technical Advisory T 5040.38. Federal Highway Administration, Washington, DC.

Flintsch, G. W., E. de León Izeppi, K. K. McGhee, and N. Shahriar, N. 2012. *The Little Book of Tire Pavement Friction*.

Hall, J., K. L. Smith, L. Titus-Glover, J. C. Wambold, T. J. Yager, and Z. Rado. 2009. *NCHRP Web-Only Document 108: Guide for Pavement Friction*. National Cooperative Highway Research Program, Washington, DC.

Henry, J. J. 2000. *NCHRP Synthesis 291: Evaluation of Pavement Friction Characteristics*. National Cooperative Highway Research Program, Washington, DC.

Highways England. 2015. *Design Manual for Roads and Bridges*. HD 28/15, Volume 7, Section 3, Part 1. Highways England, United Kingdom.

Jung, S., Jang, K., Yoon, Y., and Kang, S. 2014. Contributing factors to vehicle to vehicle crash frequency and severity under rainfall. *Journal of Safety Research*, 50, 1–10.

Meyer, W. E., R. R. Hegmon, and T. D. Gillespie. 1972. *NCHRP Report 151: Locked-Wheel Pavement Skid Tester Correlation and Calibration Techniques*. National Cooperative Highway Research Program, Washington, DC.

Noyce, D. A., H. U. Bahia, J. M. Yambo, and G. Kim. 2005. *Incorporating Road Safety into Pavement Management: Maximizing Asphalt Pavement Surface Friction for Road Safety Improvements*. Midwest Regional University Transportation Center (UMTRI), Madison, WI.

PCIS. 2013. *Accreditation and Quality Assurance of Sideways Force Skid Resistance Survey Devices*. Pavement Condition Information Systems, United Kingdom.

Quiros, S., Flintsch G.W. et al. (2018). Interconversion of Locked-Wheel and Continuous Friction Measurement. Transportation Research Record, Vol. 2672(40) 452–462

Roe, P. G., and R. Sinhal. 2005. How do you compare? Correlation and calibration of skid resistance and road surface friction measurement devices. First Inaugural International Conference on Surface Friction, Christchurch, New Zealand, May 1–4, 2005.

Tighe, S., N. Li, L. Cowe Falls, and R. Haas. 2000. Incorporating road safety into pavement management. *Transportation Research Record: Journal of the Transportation Research Board*, Vol. 1699, pp. 1–10.

TRL. 2015a. *Performance Review of Skid Resistance Measurement Devices*. Published Project Report PPR737. Transportation Research Laboratory, United Kingdom.

TRL. 2015b. *Development of a Reference Surface for the Assessment of Pavement Skid Resistance Measurement Devices*. Published Project Report PPR771. Transportation Research Laboratory, United Kingdom.

TRL. 2010. *GripTester Trial - October 2009 - Including SCRIM Comparison*. Published Project Report PPR497. Transportation Research Laboratory, United Kingdom.

THE INSTITUTE FOR TRANSPORTATION IS THE FOCAL POINT FOR TRANSPORTATION AT IOWA STATE UNIVERSITY.

InTrans centers and programs perform transportation research and provide technology transfer services for government agencies and private companies;

InTrans contributes to Iowa State University and the College of Engineering's educational programs for transportation students and provides K–12 outreach; and

InTrans conducts local, regional, and national transportation services and continuing education programs.

IOWA STATE UNIVERSITY

Visit **InTrans.iastate.edu** for color pdfs of this and other research reports.